

Diurnal brain temperature rhythms and mortality after brain injury: a prospective and retrospective cohort study

Nina M Rzechorzek (0000-0003-3209-5019), MRC Clinician Scientist Fellow¹, Michael J Thrippleton (0000-0001-7858-9917), Medical Physicist^{2,3}, Francesca M Chappell (0000-0002-7742-1757), Senior Medical Statistician³, Grant Mair (0000-0003-2189-443X), Consultant Neuroradiologist^{2,3}, Ari Ercole (0000-0001-8350-8093), Consultant in Neurointensive Care⁴, Manuel Cabeleira (0000-0002-1710-6544), CENTER-TBI Data Curator⁵, The CENTER-TBI High Resolution ICU (HR ICU) Sub-Study Participants and Investigators, Jonathan Rhodes (0000-0003-2015-4579), Consultant in Anaesthesia, Critical Care, and Pain Medicine⁶, Ian Marshall (0000-0003-4445-1551), Professor of Magnetic Resonance Physics^{2,3}, John S O'Neill (0000-0003-2204-6096),
MRC Investigator¹

Author affiliations

¹MRC Laboratory of Molecular Biology, Francis Crick Avenue, Cambridge, CB2 0QH, UK.

²Edinburgh Imaging (Royal Infirmary of Edinburgh) Facility, 51 Little France Crescent, Edinburgh, EH16 4SA UK.

³Centre for Clinical Brain Sciences, University of Edinburgh, 49 Little France Crescent, Edinburgh, EH16 4SB UK.

⁴Division of Anaesthesia, Department of Medicine, Cambridge University Hospitals NHS Foundation Trust, University of Cambridge, Box 93, Addenbrooke's Hospital, Hills Road, Cambridge, CB2 0QQ UK.

⁵Division of Neurosurgery, Department of Clinical Neurosciences, University of Cambridge, Box 167, Cambridge Biomedical Campus, Addenbrooke's Hospital, Cambridge, CB2 0QQ UK.

⁶Department of Anaesthesia, Critical Care and Pain Medicine NHS Lothian, Room No. S8208 (2nd Floor), Royal Infirmary of Edinburgh, 51 Little France Crescent, Edinburgh, EH16 4SA UK.

NOTE: This preprint reports new research that has not been certified by peer review and should not be used to guide clinical practice.

Correspondence to: Dr O'Neill at the MRC Laboratory of Molecular Biology, Francis Crick Avenue, Cambridge Biomedical Campus, Cambridge, CB2 0QH, UK, oneillj@mrc-lmb.cam.ac.uk.

ABSTRACT

Objective To determine the clinical relevance of brain temperature (T_{Br}) variation in patients after traumatic brain injury (TBI).

Design Cohort study with prospective (healthy participant) and retrospective (TBI patient) arms.

Setting Single neuroimaging site in the UK (prospective arm); intensive care sites contributing to the Collaborative European NeuroTrauma Effectiveness Research in TBI (CENTER-TBI) High Resolution ICU (HR ICU) Sub-Study (retrospective arm).

Participants 40 healthy adults aged 20-40 years recruited for non-invasive brain thermometry and all patients up to May 2020 that had T_{Br} measured directly and were not subjected to Targeted Temperature Management (TTM).

Main outcome measures A diurnal change in T_{Br} (healthy participants); death in intensive care (patients).

Results In healthy participants, mean T_{Br} (38.5 SD 0.4°C) was higher than oral temperature (36.0 SD 0.5°C), and 0.36°C higher in luteal females relative to follicular females and males (95% confidence interval 0.17 to 0.55, $P=0.0006$ and 0.23 to 0.49, $P<0.0001$, respectively). T_{Br} increased with age, most notably in deep brain regions (0.6°C over 20 years; 0.11 to 1.07, $P=0.0002$). The mean maximal spatial T_{Br} range was 2.41 (SD 0.46)°C, with highest temperatures in the thalamus. T_{Br} varied significantly by time of day, especially in deep brain regions (0.86°C; 0.37 to 1.26, $P=0.0001$), and was lowest in the late evening. Diurnal T_{Br} in cortical white matter across participants ranged from 37.0 to 40.3°C. In TBI patients ($n=114$), mean T_{Br} (38.5 SD 0.8°C) was significantly higher than body temperature (T_{Bo} 37.5 SD 0.5°C; $P<0.0001$) and ranged from 32.6 to 42.3°C. Only 25/110 patients displayed a diurnal temperature rhythm; T_{Br} amplitude was reduced in

older patients ($P=0.018$), and 25/113 patients died in intensive care. Lack of a daily T_{Br} rhythm, or an age increase of 10 years, increased the odds of death 12-fold and 11-fold, respectively (OR for death with rhythm 0.09; 0.01 to 0.84, $P=0.035$ and for death with ageing by 1 year 1.10; 1.05 to 1.16, $P=0.0002$). Mean T_{Br} was positively associated with survival (OR for death 0.45 for 1°C increase; 0.21 to 0.96, $P=0.040$).

Conclusions Healthy T_{Br} exceeds T_{Bo} and varies by sex, age, menstrual cycle, brain region, and time of day. Our 4-dimensional reference resource for healthy T_{Br} can guide interpretation of T_{Br} data in multiple clinical settings. Daily temperature variation is frequently disrupted or absent in TBI patients, in which T_{Br} variation is of greater prognostic use than absolute T_{Br} . Older TBI patients lacking a daily T_{Br} rhythm are at greatest risk of death in intensive care. Appropriately controlled trials are needed to confirm the predictive power of T_{Br} rhythmicity in relation to patient outcome, as well as the clinical utility of TTM protocols in brain-injured patients.

Registration UK CRN NIHR CPMS 42644; ClinicalTrials.gov number, NCT02210221.

SUMMARY BOX

What is already known on this topic

- Brain temperature (T_{Br}) can be measured directly in brain-injured patients via intracranial probe, but this method cannot be used in healthy individuals.
- T_{Br} can be measured non-invasively using magnetic resonance spectroscopy (MRS), but this method is not appropriate for most brain-injured patients.
- Since physiological reference ranges for T_{Br} in health have not been established, the clinical relevance of T_{Br} variation in patients is unknown, and the use of TTM in neurocritical care remains controversial.

What this study adds

- A reference map for healthy adult T_{Br} at three clinically-relevant time points that can guide interpretation of T_{Br} measured directly, or by MRS, in multiple clinical settings.
- Our results suggest that loss of diurnal T_{Br} rhythmicity after TBI increases the odds of intensive care death 12-fold; some TTM strategies may be clinically inappropriate.

INTRODUCTION

Elevated temperature has been recognized as a sign of disease for more than two millennia.¹ Both the spatial and temporal dynamics of temperature contain additional diagnostic information, exemplified by malarial fever cycles and local warming at sites of injury or infection.²⁻⁹ Internal organ temperature is rarely measured directly since invasive methods are required; in practice, temperature is assumed to be uniform throughout the brain and body core, overlooking the true clinical value of regional temperature measurements in individual tissues. Brain cell function is unequivocally temperature-dependent however,¹⁰ and it is accepted that absolute T_{Br} , its relationship to T_{Bo} , and the apparent temperature-sensitivity of brain tissue are frequently altered following injury.^{3,7,8,11,12} Indeed, understanding of human T_{Br} has largely been informed by studies of brain-injured patients, where intracranial probes allow precise ($\pm 0.1-0.3^\circ\text{C}$), direct measurement from a single brain locus.^{13,14}

The temperature-dependence of brain function has perpetuated the assumption that T_{Br} must be relatively homogenous and static in health. However, several lines of evidence suggest that T_{Br} may vary over time, and between brain regions.^{4-5,7,9,11,12,15-19} For example, human core T_{Bo} is 1-2°C lower during sleep at night, when cerebral blood flow is also ~20% higher^{20,21}; therefore, brain heat removal should be more efficient at night than during the day. Moreover, direct measurements in non-human primates show that deep brain structures are warmer than the brain surface, and that T_{Br} varies at least as much as T_{Bo} across a 24-hour period.^{18,19}

Establishing how T_{Br} varies in health is critical; deviations from normal may have transformative diagnostic and/or prognostic value in neurological disease and injury, but only if these deviations can be distinguished from physiological variation over time.²² With magnetic resonance spectroscopy (MRS), spatially resolved T_{Br} data can now be obtained through non-invasive brain imaging.¹³ Brain thermometry has proven to be a powerful research application of MRS but, with respect to healthy humans, it has only been used in studies that were poorly controlled for parameters that influence physiological temperature variation (Supplementary Table S1). We sought to establish the daily spatiotemporal variation of healthy T_{Br} to enable evidence-driven appraisal of the clinical value of T_{Br} monitoring in brain-injured patients. We hypothesized that healthy T_{Br} would vary diurnally, and that disruption of diurnal temperature variation would be associated with outcome after TBI.

METHODS

Reporting adheres to STROBE guidelines.

Prospective study design and recruitment

We conducted a prospective, single-site, cohort study in healthy adults, controlled for age, sex, body mass index (BMI), menstrual cycle phase, seasonal variation, and individual chronotype. Our primary objective was to determine whether healthy T_{Br} varies by time of day. Our secondary objectives were to compare variability in brain and oral temperatures, to test for differences between males and luteal-phase females, and explore brain-regional changes in T_{Br} with time. We hypothesized that T_{Br} would (i) exceed and vary more than oral temperature across the day, (ii) be higher in luteal females relative to males, and (iii) increase with increasing brain tissue depth. Sample size was estimated for achieving the primary outcome (a change in mean global T_{Br} between time points) using a linear mixed model, considering published data on the reliability of MRS brain thermometry in healthy men.¹³ With 36 subjects, and a conservative true mean T_{Br} difference of

0.5°C, we estimated 80% power to detect a statistically significant difference between time points at the 5% significance level. A health-related finding (HRF) on MRI was the key exclusion criterion. Completion of a feedback pathway for two volunteers was expected (based on 5% prevalence of HRFs using high-resolution MRI).²³ We aimed to scan 40 eligible participants (20 females) to account for potential withdrawal, exclusion, and/or technical scan failure.

Recruitment for our Circadian Brain Temperature (CiBraT) Study was based on meeting criteria for our primary outcome (Supplementary Table S2), and was conducted locally using mailshots to University of Edinburgh and NHS staff, social media posts, and posters displayed at University of Edinburgh campuses and NHS Lothian hospitals. By completing an online eligibility questionnaire, all prospective participants provided written informed consent for their personal data to be used to schedule consenting interviews, and to notify general practitioners of their intention to participate. The questionnaire provided access to inclusion and exclusion criteria, the Participant Information Sheet and Consent to Participate Form (Supplementary Appendix 1), and Data Protection Information sheet. All participants provided written, informed consent to participate during face-to-face interview conducted by the Chief Investigator (NMR) at the University of Edinburgh. Additional written informed consent was obtained for publication of individual data which, by nature of its distinctive features, could potentially be recognized by participants as their own data. The Study Protocol is presented in Supplementary Appendix 2.

Prospective data collection

During a consenting interview at the study site, one week in advance of scanning, each participant was given a wrist-worn actimeter (ActTrust2, Condor Instruments, Sao Paulo, Brazil). Each participant then underwent three identical brain scans in the morning (9-10am), afternoon (4-5pm), and late evening (11pm-midnight) of their scheduled scanning day. Multiple time points spanning >12 hours were selected because the human circadian rhythm (body clock) impacts almost every

aspect of physiology (Supplementary Text '*Internal rhythms and health*').²⁴⁻²⁷ The exact alignment, or phase relationship, between the body clock and the day-night cycle is dictated by individual chronotype, which is determined by genetic and lifestyle factors, and can be derived from longitudinal monitoring of locomotor activity.²⁸ To assign scan times to the appropriate part of each participant's circadian cycle, we determined individual chronotypes using wrist actigraphy to extract the sleep-corrected midpoint of sleep on free (non-work) days (MSF_{sc}) (Supplementary Methods).²⁸ Height and weight were measured immediately before the morning scan to calculate BMI. Oral temperature was recorded before each scanning session using a digital Clinical Thermometer (S.Brannan & Sons, UK) covered in a single-use Probe Cover (Bunzl Retail & Healthcare Supplies Limited, Middlesex, UK) and placed sublingually. For females, hormonal influences were controlled through urine-based ovulation testing (ClearBlue®), or documenting hormonal contraception type. We aimed to scan females during the luteal phase of their natural menstrual cycle, or on a day when an active combined pill would be taken, or combined patch worn. Females using other forms of contraception (implant or intrauterine device) were excluded. On the day of scanning, food consumption was restricted to 6am–8am, 12noon to 2pm, and 6pm–8pm, and caffeine consumption was restricted to 6am–8am and 12noon to 2pm. Alcohol was strictly prohibited at all times. Participants were asked not to participate in excessive physical activity on the day of scanning. Data collection was limited to a 14-week period between July and October 2019 to avoid daylight savings clock changes and large seasonal variation in environmental light and temperature conditions. Data management procedures are described in Supplementary Methods.

Brain imaging

All brain imaging was conducted at the Edinburgh Imaging (Royal Infirmary of Edinburgh) Facility using a 3-T MAGNETOM Prisma scanner (Siemens Healthcare, Erlangen, Germany) with a 32-channel head coil. All participants were screened for MRI contraindications and changed into

hospital scrubs for each scanning session—conducted in a temperature-controlled room (target 21.5°C). Room lights were off and the scanner lighting and fan were maintained on their lowest setting. Ear protection was provided and a mirror was attached to the head coil so participants had the choice of closing their eyes or viewing the MRI control room; no visual or acoustic entertainment was provided. Participants were permitted to sleep during scans and were asked to report on this event at the end of each session. At each time point, after whole-brain structural MRI, MRS data were collected from 82 brain locations (voxels). The scanning protocol was well tolerated, with no serious adverse events reported during 7-day follow-up. Further details on the scanning protocol and MRS data processing are provided in Supplementary Methods and Appendix 3; the dedicated Study Participant Data Form (Case Report Form) is provided in Appendix 4.

Calculation of MRS-derived brain temperature

MRS brain thermometry exploits the fact that the chemical shift of water is exquisitely temperature-dependent (-0.01ppm/°C), whilst that of the reference metabolite NAA is not.²⁹ The chemical shift difference between water and NAA can estimate absolute T_{Br} in healthy men with a short-term precision of 0.14°C at 3-T.¹³ T_{Br} for each brain tissue voxel in this study was calculated using the following relationship:

$$T_{Br} = 100 * [\text{NAA frequency} - \text{H}_2\text{O frequency} + 2.665] + 37$$

where frequency is in ppm and temperature is in °C

The reliability and accuracy of T_{Br} determination using this MRS protocol was thoroughly tested using *in vivo* human and *in vitro* phantom measurements; the latter validated with an MR-compatible industrial thermometer that meets international standards.¹³

Retrospective study design and patient data sources

To determine the clinical relevance of T_{Br} variation, we conducted a multicentre, retrospective cohort study of TBI patients that had high temporal-resolution T_{Br} data collected directly from the brain.

Data for all eligible patients were extracted using version 2.0 of the CENTER-TBI dataset, compiled between 2015 and 2017. Additional eligible patients monitored at one of the contributing sites (the Intensive Care Unit, Western General Hospital, Edinburgh, UK) were included up to May 2020 and comprised 109 of the 134 eligible patients screened. The Western General Hospital is the tertiary referral centre in South East Scotland for neurosurgical emergencies. Patients with moderate to severe TBI admitted to intensive care requiring intubation, sedation, and intracranial pressure (ICP) management also received brain oxygen tension and temperature monitoring using the Integra Licox system (Integra, France). Patients were managed in accordance with Brain Trauma Foundation guidelines.³⁰ Patients were either admitted directly to intensive care or following surgical intervention for mass lesions. T_{Br} was measured via a thermistor, inserted into the brain parenchyma via a dedicated bolt placed via a burr hole (Integra Neurosciences, Andover, UK). The bolt was placed so that the thermistor inserted into frontal white matter; for diffuse injuries this was into the non-dominant hemisphere. When the main injury was focal, the bolt was placed on the side of maximal injury, unless this would place the monitors into non-viable tissue. High temporal-resolution physiological data were recorded at a minimum of 1-minute intervals to either a bedside computer running ICU Pilot software (CMA, Sweden) or to a Moberg neuromonitoring system (Moberg Research Inc., USA). Data were collected continuously (except for interruptions due to computed tomography scanning or surgical intervention) and until ICP monitoring was no longer required, or the patient died. Data for the CENTER-TBI study were collected through the Quesgen e-CRF (Quesgen Systems Inc, USA), hosted on the INCF platform and extracted via the INCF Neurobot tool (INCF, Sweden). For patient monitoring and data collection in the High-Resolution repository, the ICM+ platform (University of Cambridge, UK) and/or Moberg Neuromonitoring

system (Moberg Research Inc., USA) were used. For T_{Bo} , the primary method of measurement was documented in 26 of 134 screened patients and included tympanic (21), bladder (3), external axillary (1), and nasopharyngeal (1). Secondary sites included rectal, external axillary, oesophageal, and skin.

Patient temperature data processing

Four inclusion criteria levels were applied to ensure that sufficient temperature data were available to assess for a diurnal rhythm (Table 1), and that any data potentially affected by TTM protocols were excluded. Analysis of patient temperature data was blinded to outcome. Data from the first 2 hours of monitoring were excluded from the analysis to ensure the results were not influenced by the time required for the electrode to stabilise. Raw data processing was performed in Excel to exclude artefactual data, identify any gaps in the time series, and define the analysis window. Temperature data were visualized in GraphPad Prism version 8.2 and assessed for the presence of daily rhythmicity. Visual analyses were validated with a combination of rhythm-detection algorithms using GraphPad Prism, BioDare2 (biodare2.ed.ac.uk)³¹ and the Harmonic Regression package in R.³² To be categorized as diurnally rhythmic, the patient's temperature pattern need not be conventionally aligned with the day-night cycle, but it had to meet both of the following criteria:

- (1) a period length of ~22–26h in at least part (but not necessarily all) of the time series as determined by blinded visual analysis of the raw data in GraphPad Prism and
- (2) a period length of 22-26h as determined by period analysis in (i) cosinor analysis in GraphPad Prism and/or (ii) statistically significant output from Harmonic Regression in R and/or (iii) BioDare2.

In GraphPad Prism, period results were only considered valid if a cosinor curve fit was significantly preferred over a straight line. When using the Harmonic Regression package, the period length term (Tau) of the model to test for was set to 24 hours. In BioDare2, period analysis was performed using

6 different algorithms. A full description of these algorithms can be found at <https://biodare2.ed.ac.uk/documents/period-methods>.

<p>Level A: Criteria for extracting maximum and minimum daily brain and/or body temperatures</p> <ul style="list-style-type: none"> • Known sex • Known age • Minimum 24 hours of temperature data collection under ‘constant’ conditions. The first data point recorded in the intensive care setting that exceeds the minimum recorded temperature from that patient in the absence of TTM will be taken as the start point (to exclude low temperature points surrounding insertion of probe or those relating to patient hypothermia on arrival in intensive care) • For data where only the maximum and minimum daily T_{Bo} (and in some cases T_{Br}) are recorded with their respective times, a minimum of two days’ worth of data is needed • If TTM was applied, only data relating to time preceding TTM or after the first inflection of data after cessation of TTM can be used and must meet the above requirements for minimum time length in the absence of TTM • When extracting the time of the minimum and maximum temperature point, the first occurrence of that specific temperature point under intensive care ‘constant’ conditions will be selected
<p>Level B: Additional criteria for performing diurnal rhythmic temperature analyses</p> <ul style="list-style-type: none"> • Minimum hourly T_{Bo} or T_{Br} data with T_{Br} data extracted via intracranial probe (standard depth and positioning in cortical white matter) recorded continuously over a minimum of 36 hours. The same rules as above apply in relation to TTM. • Ideally minimum hourly data of another matched parameter (ICP, $PbTO_2$, MAP) with expected diurnal rhythm
<p>Level C: Additional criteria for correlation with outcome</p> <ul style="list-style-type: none"> • Mortality/survival in intensive care • Ideally GOSE at 3 and/or 6 months (imputed where necessary)
<p>Level D: Additional criteria for correlation with injury severity</p> <ul style="list-style-type: none"> • One of more of the following parameters: presence of pupillary light reflex in one/both/no eyes; GCS, GCSM • Ideally injury type (focal/diffuse; from CT scoring) and/or severity (IMPACT imputed GCS) on admission to Study Hospital and/or TIL score (including individual components of this) • Ideally site of probe insertion for focal injury (ipsilateral or contralateral to injury—to be determined using CT/MRI images if available)

Table 1. Inclusion criteria for retrospective analysis of temperature data from TBI patients.

TTM, Targeted Temperature Management; ICP, Intracranial pressure; $PbTO_2$, partial pressure of brain oxygen; MAP, mean arterial pressure, CT, computed tomography; MRI, Magnetic Resonance Imaging; IMPACT, International Mission for Prognosis and Analysis of Clinical Trials in TBI; GCS, Glasgow Coma Score, GCSM, Glasgow Coma Score Motor response; TIL, Therapy Intensity Level; GOSE, Glasgow Outcome Scale Extended.

Statistical analysis

To determine healthy temperature variation, we applied a linear mixed modelling approach. The fixed effects (predictors) were specified *a priori* based on published literature describing factors that were most likely to affect body and/or brain temperature in humans and other mammals.²² In each case, the upper limit for the number of fixed effects was set to a maximum of five to avoid over-fitting each model within the confines of our sample size.³³ Random effects for intercept and slope were included, allowing participants to have different baseline temperatures and different changes in temperature over time. The models for oral temperature (*OralTemp*) and T_{Br} (*BrainTemp*) were built as follows:

$$OralTemp_{ij} = [intercept (\beta_0) + Time (\beta_1) + Sex (\beta_2) + EdTemp (\beta_3) + Age (\beta_4) + BMI (\beta_5)] + \varepsilon_{ij}$$

(residuals for subject i at time j) + $U1i$ (intercept for subject i) + $U2i$ (slope for subject i in relation to Time)

where fixed effects include:

Time (time of day normalized for chronotype using the ‘time distance’ between the T_{Oral} measurement and MSF_{sc} for that participant as a proportion of a linearized unit circle where 0= MSF_{sc} and 1=24 hours)

Sex (participant biological sex categorized as male, luteal female, or non-luteal female)

EdTemp (environmental temperature in Edinburgh on that date and at the time of temperature measurement)

Age (participant age on date of temperature measurement)

BMI (participant BMI on date of temperature measurement)

with random effects for intercept by subject, and for slope by subject with respect to Time

$$\begin{aligned} BrainTemp_{ij} = & [intercept (\beta_0) + Time (\beta_1) + Sex (\beta_2) + BrainRegion (\beta_3) + Age (\beta_4) + Sleep (\beta_5)] \\ & + \varepsilon_{ij} \text{ (residuals for subject } i \text{ at time } j) + U1_i \text{ (intercept for subject } i) + U2_i \text{ (slope for subject } i \text{ in} \\ & \text{relation to time)} \end{aligned}$$

where fixed effects include:

Time (time of day normalized for chronotype using the ‘time distance’ between the T_{Br} measurement and MSF_{sc} for that participant as a proportion of a linearized unit circle where 0= MSF_{sc} and 1=24 hours)

Sex (participant biological sex categorized as male, luteal female, or non-luteal female)

BrainRegion (brain voxel categorized to one of six regions: Superficial 1, Superficial 2, Superficial 3, Superficial 4, Thalamus, Hypothalamus)

Age (participant age on date of temperature measurement)

Sleep (whether participant reported falling asleep during scanning; categorized as ‘yes’, ‘maybe’ or ‘no’)

with random effects for intercept by subject, and for slope by subject with respect to Time

To confirm that there was no relationship between T_{Br} and BMI, the model was run a second time, but replacing the *Sleep* effect with *BMI*. The model for deep T_{Br} was identical to the *BrainTemp* model above except that only thalamic and hypothalamic regions were included (Supplementary Appendix 5).

For retrospective data, a generalized linear mixed model (GLMM) for logit binomial distribution of patient outcome was chosen (the rationale for model choice is provided in Supplementary Methods). Survival in intensive care or ‘alive’ was specified as a miss, and death or ‘dead’ as a hit. The model incorporated fixed effects and random effect for intercept and was built as follows:

$$Outcome_i = [intercept (\beta_0) + Age (\beta_1) + Sex (\beta_2) + BrainMean (\beta_3) + BrainRange (\beta_4) + Diurnal (\beta_5)] + \varepsilon_{ij} \text{ (residuals for patient } i) + UI_i \text{ (intercept for patient } i)$$

where fixed effects include:

Age (patient age in intensive care)

Sex (patient biological sex categorized as male or female)

BrainMean (absolute mean T_{Br} throughout analysis window)

BrainRange (T_{Br} range across analysis window)

Diurnal (presence or absence of a daily temperature rhythm within analysis window—categorized as ‘yes’ or ‘no’; see above for details on how tests for diurnal rhythmicity were performed)

with random effects for intercept by subject

The final choice of fixed effects (predictors) to include in the model was based on our core study objectives, avoiding redundant terms, and optimising the model fit (Appendix 5). Missing data values for any of the model components were input as ‘NA’, and thus patients with values missing for one or more of the components were excluded from the model output. The most conservative approach was taken i.e. multiple imputation was not performed since the random nature of missing data could not be assumed.

Statistical modelling and other circular analyses were performed using R version 3.6.3 (R Core Team, 2020) and the circular (v0.4–93; Lund et al., 2017); cosinor (v1.1; Sachs 2015), cosinor2 (v0.2.1; Mutak 2018), lme4 (v1.1–23; Bates et al. 2020), effects (v4.1-4; Fox et al. 2019), afex (Singmann et al., 2020), Matrix (v1.2-18; Bates et al., 2019), Cairo (v1.5-12.2; Urbanek and Horner 2020), yarr (v0.1.5; Phillips 2017) and car (v3.0-8; Fox et al., 2020) packages. The full reproducible code is provided in Supplementary Appendix 5, or is available on request to the Lead Author. All other analyses were performed in GraphPad Prism version 8.2.

Patient and public involvement

Edinburgh Imaging staff were actively involved in the design of the prospective study. Pre-existing patient temperature data helped to inform the selection of most appropriate time points for scanning in healthy participants. TBI patients were not actively involved in study design since their data was anonymised prior to extraction and analysis. Healthy participants were invited to outline reasons for non-willingness to participate; where appropriate, this information was used to refine the recruitment approach. The findings of this study will be disseminated via Open Access publication. Conference presentations and public engagement activities will be used to explain the purpose of the research and its potential future impact. End of Study Information Sheets will be emailed to individual healthy participants who gave consent to receive these, and a lay summary of the study results will be posted online after publication.

RESULTS

Spatiotemporal measurements of healthy brain temperature

Of the 77 volunteers screened for eligibility, we recruited 20 males and 20 females (aged 20–40 years) between July and September 2019 (Fig.1A). Participants represented 15 nationalities across five continents, and the last participant was scanned on October 8th 2019. One male attended only for morning scanning and another male volunteer missed afternoon scanning; available data from both of these participants was included in the analysis. Of the females scanned, 11 had natural menstrual cycles, eight were taking a combined contraceptive pill and seven of these took an ‘active’ pill on the day of scanning. The female subject on a ‘pill break’ reported day one of menstruation at their afternoon scan; their T_{Br} data was included in the luteal group. Of the females with natural cycles, six were confirmed luteal (urine test), two were in menstruation, and three were in non-menstrual follicular phase at scanning. Five females thus formed a non-luteal group. One female wore a

combined contraceptive patch on the scanning day (transiently removed during each scan); their T_{Br} data was included in the luteal group (fig.S5).

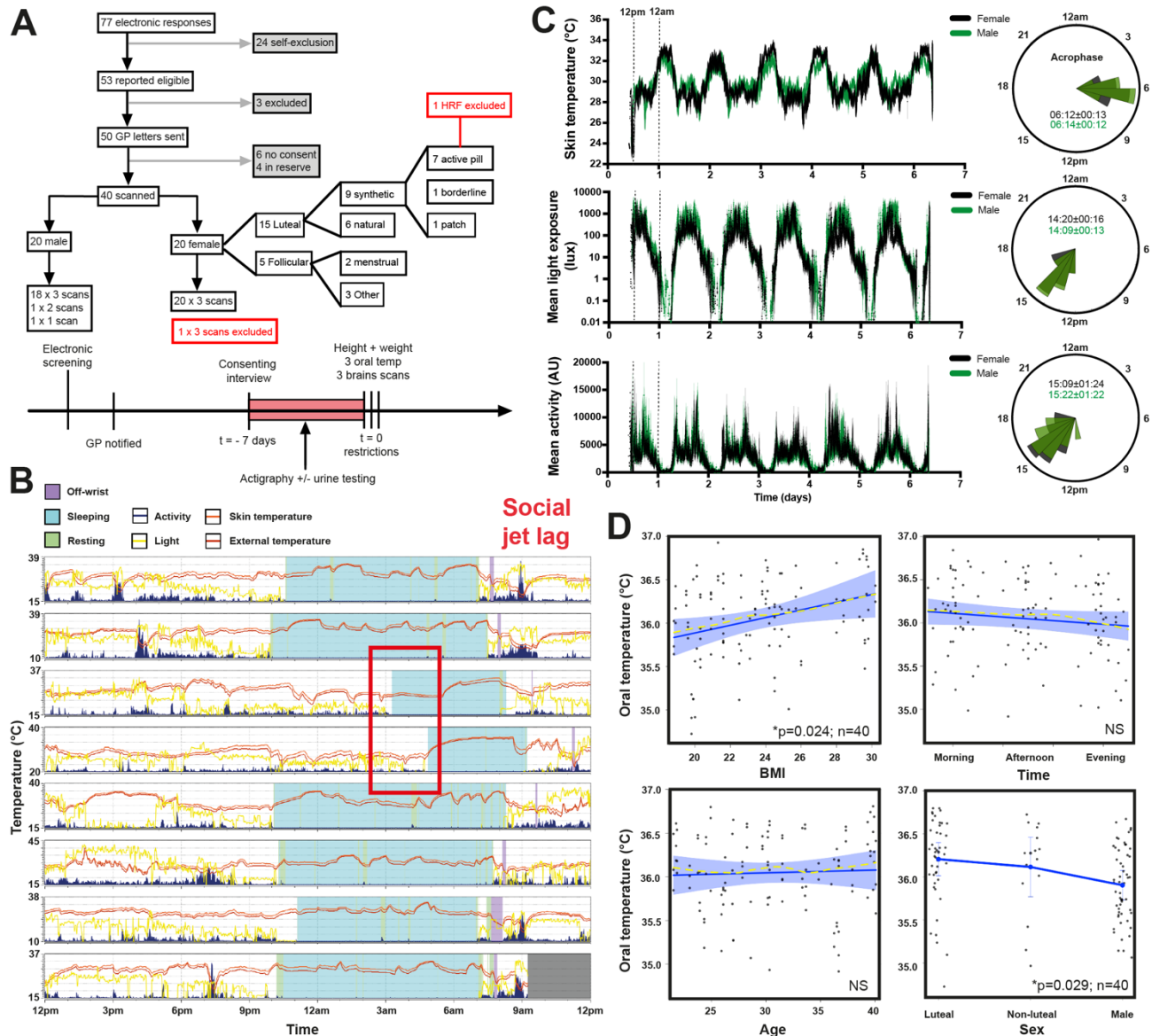


Fig. 1. Chronotype-controlled temperature variations. (A) Prospective study profile and workflow. (B) Representative actogram displaying typical actigraphy over one week from one male volunteer. Horizontal panels represent consecutive days. Note absence of light exposure and activity, with increase in skin temperature during sleep time (activity also absent when device was ‘off-wrist’). Social jet lag refers to large delay in sleeping schedule due to social activities on two consecutive days, highlighted (red box). (C) Group-averaged mean±SEM data for distal skin (wrist)

temperature, total light exposure, and activity by sex during actigraphy week (left). Females n=20, males n=20. Associated rose plots with circular means (acrophases \pm SD) displayed (right). For each data type, radial uniformity was rejected for both groups (Rayleigh uniformity test $p < 0.0001$) and there were no significant differences in circular mean between them (Watson's two-sample test for homogeneity, $p > 0.1$). (D) Linear mixed modelling results for oral temperature. Solid blue lines represent model fits, shaded areas and double-ended error bars represent 95% confidence intervals, dark grey circles display residuals (single temperature data points), and smoothed dashed yellow lines represent partial residuals. The x-axis for Time summarizes the continuous variable of time distance since the participant's MSF_{sc} (proportion of a linearized unit circle, where 0=MSF_{sc} and 1=24 hours). Note time-dependent trend but lack of significant diurnal variation in oral temperature, likely reflecting inherent practical challenges of obtaining accurate oral temperature readings in human subjects.³⁴

All subjects exhibited diurnal variation in wrist skin temperature, which was anti-phasic with their rhythm in activity and light exposure, in the week preceding their scans (Fig.1B-C and fig.S1-S2). BMI was marginally higher in males ($P=0.014$; Table 2). Oral temperature was 0.29°C higher in luteal females relative to males (95% confidence interval 0.03 to 0.58, $P=0.029$), and 0.04°C higher for a unit increase in BMI (0.005 to 0.083, $P=0.024$; Fig.1D). There were no differences in oral temperature by age or time of day however, despite daily changes in environmental temperature (Fig.1D, fig.S3). Brain locations for MRS data sampling are shown in Fig.2A. MRS data from one female were excluded due to a HRF; 24 T_{Br} data points from a total of 9434 (0.25%) were excluded because they did not meet quality control criteria for MRS spectral fitting (Supplementary Methods, fig.S4, Table S3). The data points that failed quality control derived from 15 of the 40 subjects scanned. Together, these data confirmed that our cohort was representative of healthy adult men and women with respect to basic physiological parameters, chronotype distribution, and sleep patterns.

Our novel chronotype-controlled imaging protocol reproducibly obtains time-resolved T_{Br} data at high spatial resolution.

	Females (n=20)	Males (n=20)
Age (y)	29.76 (5.48)	31.81 (6.16)
BMI	22.33 (2.80)	24.97 (3.65) [†]
No. days actigraphy data		
Free	1.6 (1.23)	1.65 (1.50)
Scheduled	6.0 (1.26)	5.95 (1.73)
Total	7.6 (0.60)	7.6 (0.94)
Sleep onset	23:33 (00:55)	23:59 (01:07)
Onset latency (min)	5.4 (4.26)	4.4 (2.33)
Sleep offset	07:40 (00:50)	07:50 (01:04)
Sleep duration (min)	486.5 (33.47)	474.2 (39.61)
Total sleep time per night (min)	442.4 (34.95)	424.8 (37.00)
WASO (min)	40.05 (17.90)	43.80 (22.07)
Sleep efficiency (%)	89.93 (3.86)	89.04 (4.99)
MSF_{sc}	03:56 (01:01)	03:58 (01:26)
MSW_{sc}	03:33 (00:50)	03:53 (01:01)
PCSM	03:15 (00:34)	03:31 (01:17)
SJL_{sc} (min)	52.27 (49.28)	38.82 (34.06)
Acrophase	15:09 (01:24)	15:22 (01:22)
CFI	0.65 (0.07)	0.67 (0.08)
Oral temperature (°C)		
Morning	36.18 (0.51)	36.02 (0.40)
Afternoon	36.11 (0.60)	36.03 (0.48)
Evening	36.09 (0.57)	35.84 (0.43)
MRI room temperature (°C)		
Morning	21.02 (0.67)	21.36 (0.76)
Afternoon	21.98 (0.63)	21.94 (0.71)
Evening	21.30 (0.64)	21.38 (0.53)
Scan duration (minutes)		
Morning	31.80 (3.82)	31.10 (3.29)
Afternoon	30.50 (6.68)	29.61 (2.97)
Evening	29.55 (2.09)	28.63 (1.64)
Slept during scan		
Morning	1 (0)	2 (3)
Afternoon	6 (1)	6 (2)
Evening	5 (0)	5 (1)

Table 2. Healthy participant demographics and sleep characteristics. Data presented as arithmetic mean (SD) except for Sleep Onset, Sleep Offset, and Acrophase (where circular mean (SD) is presented) and ‘slept during scan’ where numbers of individuals are presented as definite (possibly). Mean calculated across entire data collection period for each participant prior to calculation of group mean, where applicable. [†]BMI higher in males than females (P=0.014; unpaired

two-tailed t-test with Welch's correction). Sleep onset = bed time plus latency of sleep onset. Sleep offset = wake up time. Sleep duration = duration between sleep onset and offset. Total sleep time = total duration of sleep period after removing periods of wakefulness. WASO = wake after sleep onset time (refers to periods of wakefulness occurring after defined sleep onset; a reflection of sleep fragmentation). Sleep efficiency = the percentage of time spent asleep while in bed. Calculated by dividing the amount of time spent asleep by the total amount of time in bed. A normal sleep efficiency is considered to be 80% or higher. MSF_{sc} = sleep corrected midpoint of sleep on free days (sleep onset on free days plus half of the average weekly sleep duration for all days). MSW_{sc} = sleep corrected midpoint of sleep on work days (sleep onset on work days plus half of the average weekly sleep duration for all days). PCSM = previous corrected sleep midpoint (sleep corrected midpoint of sleep on the night before scanning). SJL_{sc} = sleep corrected social jetlag ($MSF_{sc} - MSW_{sc}$ or absolute difference between sleep onset on free and work days when average sleep duration was longer on free than work days; if average sleep duration was longer on work days than free days, SJL_{sc} was calculated as the absolute difference between sleep offset on free and work days). Note that this parameter was calculated only for participants that reported at least one of each 'day type' (free or scheduled) during data collection. CFI = circadian function index; this parameter ranged from 0.43–0.73 in an age-matched group of healthy volunteers.³⁵

Regional variation in brain temperature by sex and age

Global T_{Br} was higher than oral temperature (38.5 SD 0.4°C versus 36.0 SD 0.5°C), and was 0.36°C higher in luteal females relative to follicular females and males (95% confidence interval 0.17 to 0.55, $P=0.0006$ and 0.23 to 0.49, $P<0.0001$, respectively). This sex difference appeared to be driven by menstrual cycle phase (fig.S5). Despite age-selective recruitment, we captured an age-dependent increase in T_{Br} , most notably in deep brain regions (thalamus and hypothalamus; 0.6°C over 20 years; 0.11 to 1.07; $P=0.0002$). Sex, age, and spatial effects on T_{Br} are summarized in Fig.2B and

Fig.S6A. The mean maximal spatial T_{Br} range (difference between hottest and coolest voxel in an individual at any given time point) was 2.41 SD 0.46°C. In the cerebrum, white matter-predominating areas were relatively warm. The lowest temperatures were observed in cortical grey matter regions lying close to the brain surface and adjacent to a major venous drainage channel (region Sup1, surrounding the superior sagittal sinus). The highest temperatures were observed in the thalamus (1.64°C higher than cortical grey matter, 1.57 to 1.72, $P < 0.0001$; 0.56°C higher than hypothalamus, 0.39 to 0.73, $P < 0.0001$). Eight female and 12 male participants reported having ‘definitely’ or ‘possibly’ fallen asleep during one or more scans; this had no measurable impact on T_{Br} within the 30-minute scan time (Appendix 5). Collectively, these data show that normal human T_{Br} substantially exceeds oral temperature and varies by sex, age, menstrual cycle, and brain region.

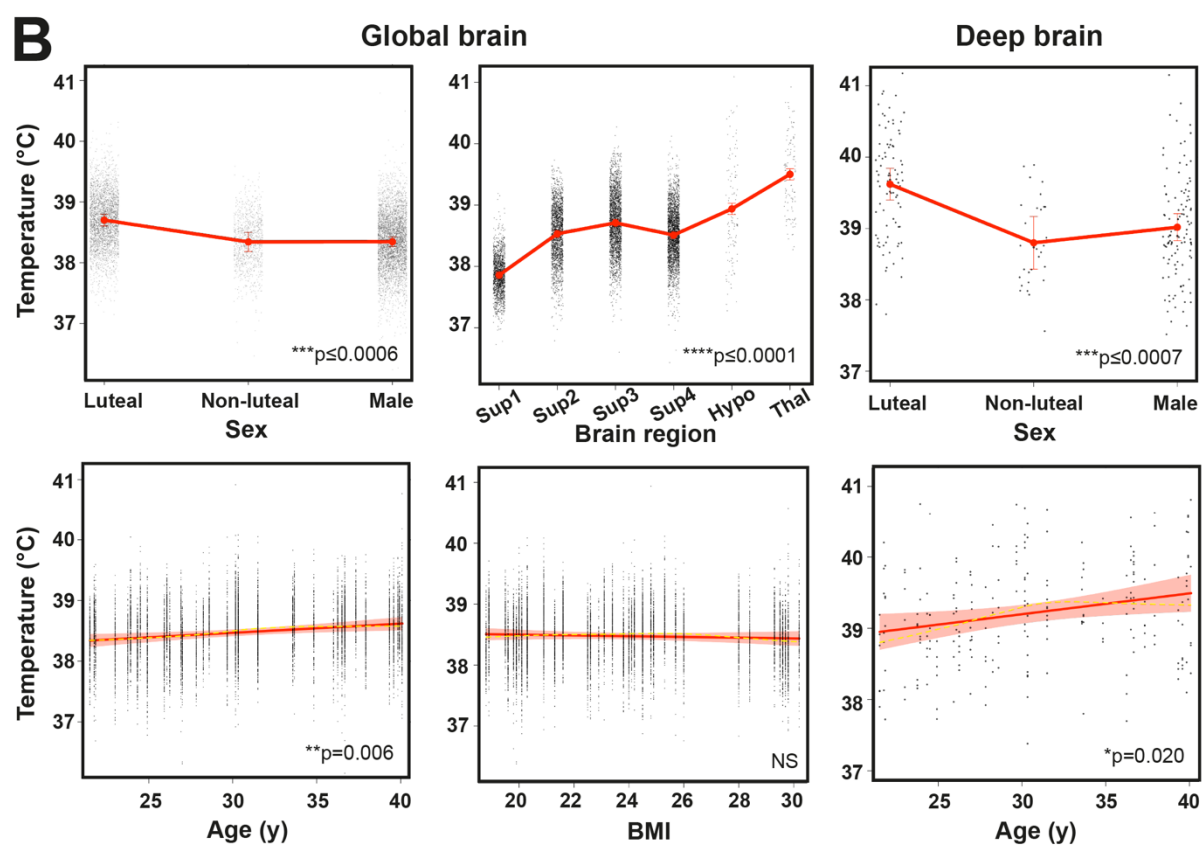
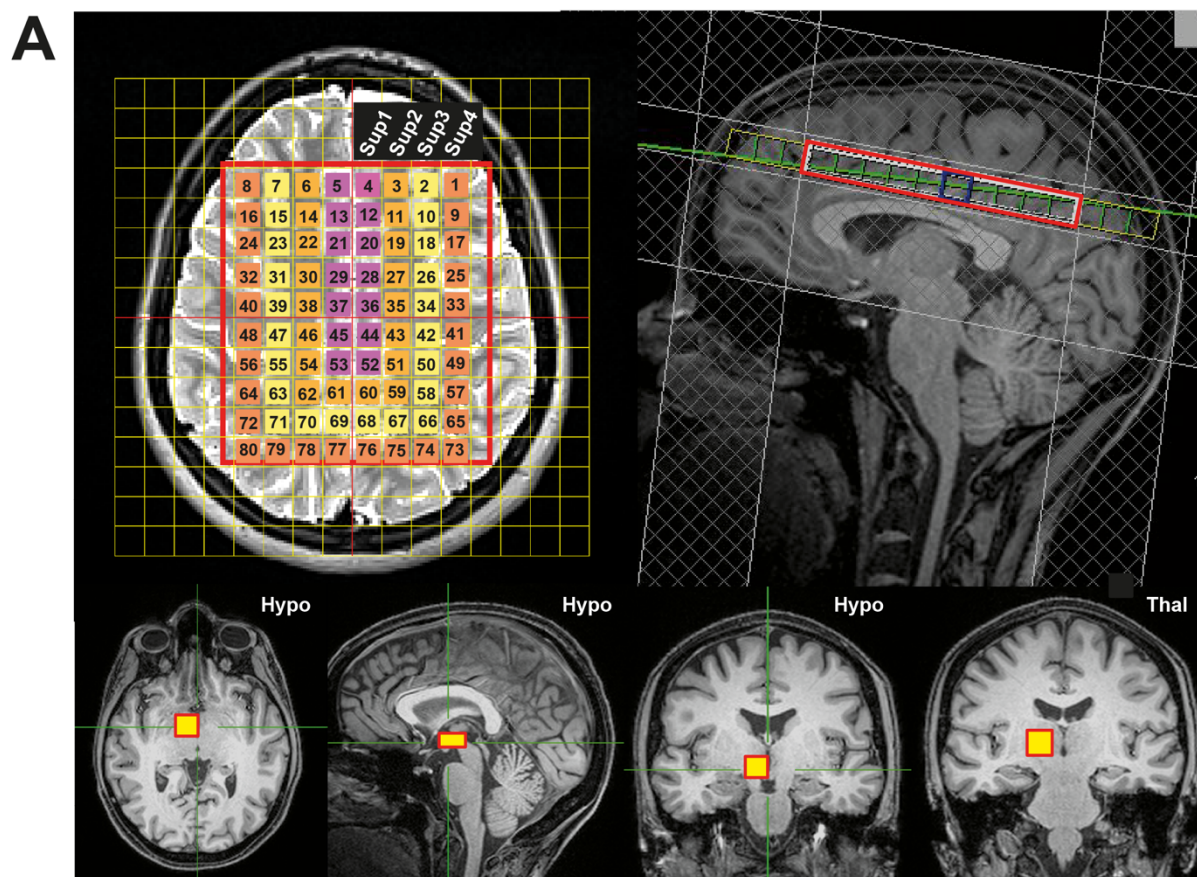


Fig. 2. Human T_{Br} is spatially heterogenous. (A) Representative annotated MR images to show MRS extraction protocol immediately after whole-brain structural acquisition. T2-weighted axial (top left) and T1-weighted mid-sagittal (top right) image showing multivoxel MRS overlay for more superficial brain regions including cerebral grey and white matter; note positioning superior to corpus callosum. From this multivoxel acquisition, MRS data was extracted from each of the numbered voxels individually; for the final statistical model, the whole cerebral region was split into 4 superficial groups of voxels (Sup1–4, depicted as separate colours in the overlay, from medial to lateral). T1-weighted axial, sagittal, and coronal images (bottom three images from left side, respectively) showing orthogonal positioning of single voxel in right hypothalamus (yellow box). T1-weighted coronal image (bottom right) showing positioning of single MRS voxel in right thalamus (yellow box). (B) Linear mixed modelling results for global T_{Br} by sex, age, brain region, and BMI, and for deep T_{Br} (including thalamus and hypothalamus) by sex and age. Solid red lines represent model fits, shaded areas and double-ended error bars represent 95% confidence intervals, dark grey circles display residuals (single temperature data points), and smoothed dashed yellow lines represent partial residuals. For sex, P-value reflects comparisons of each group with luteal females. For brain region, P-value represents comparisons of each region relative to superficial region 1 (parasagittal group of voxels). Sup1–4, superficial brain regions 1–4 from medial to lateral; Hypo, hypothalamus; Thal, thalamus.

Diurnal variation in brain temperature

Absolute T_{Br} is ultimately determined by a balance between the rate of heat generated by the brain, and its rate of heat loss, mediated principally by CBF.^{36,37} Since blood arrives to the brain from the body at a lower temperature, this temperature gradient should enable effective brain heat removal, as long as cerebral perfusion is maintained.³⁸ It follows that T_{Br} must be partially determined by T_{Bo} . Since T_{Bo} and CBF both show clear diurnal regulation in humans, with lower temperature and higher CBF at night,^{20,21} we reasoned that human T_{Br} should drop in the evening. Our linear mixed model (Fig.3A-B) revealed that global T_{Br} varied by 0.57°C (95% confidence interval 0.40 to 0.75, $P<0.0001$) across time; whereas deep brain varied by 0.86°C (0.37 to 1.26, $P=0.0001$) and the hypothalamus displayed the greatest temporal variation (1.21 SD 0.65°C , range 0.27 to 2.75°C). Diurnal temperature variation was significantly greater in deep brain regions than in the cerebrum or the body (oral temperature; Fig.3C and fig.S6B-C), and for all brain regions, T_{Br} was lowest in the late evening. Robust, approximately sinusoidal, daily T_{Bo} rhythms are a very well-characterised aspect of human physiology, and similar temperature rhythms have been extensively documented in other diurnal mammals in the brain and body.^{39,40} Since T_{Br} is expected to depend (at least in part) on T_{Bo} , we used the simplest and most appropriate mathematical model (cosinor analysis) to predict diurnal human T_{Br} in a continuous fashion. We interpolated a sinusoidal time series for T_{Br} in six brain regions of interest (Fig.3D). The predicted average minimum (anticipated around MSF_{sc} , ~3am) was 38.4°C in luteal females and 38.0°C in males. Importantly, the diurnal T_{Br} range across individuals was ~ 37.0 – 40.3°C in healthy cortical white matter—the location measured in patients with moderate-to-severe brain injury. In summary, these data show that normal human T_{Br} varies substantially over the day, in a sex- and brain region-dependent fashion.

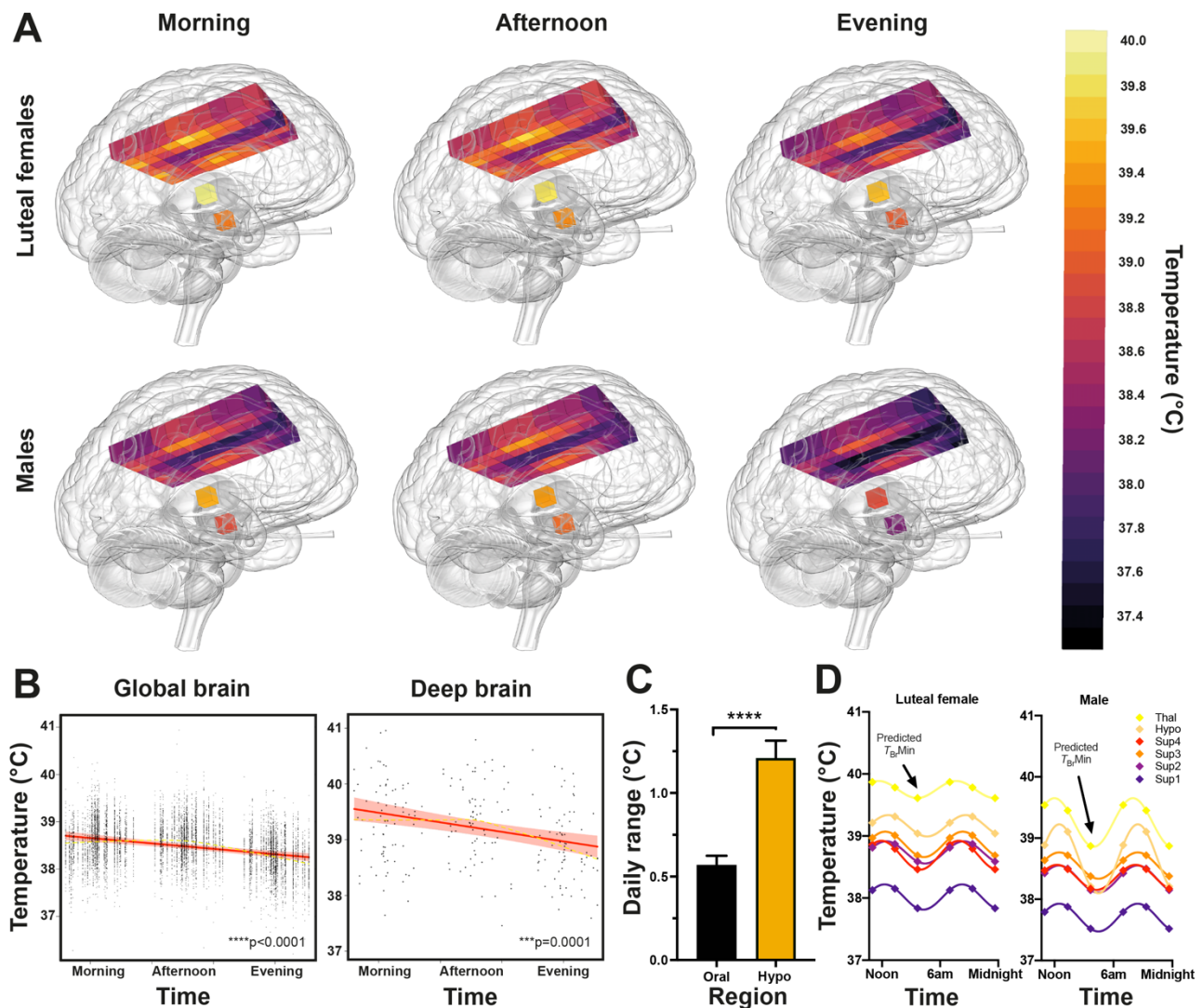


Fig. 3. Human T_{Br} varies by time of day. (A) Snapshot 3D maps of T_{Br} at each data collection point. Inferno colour scale is used to assign a temperature to each tissue voxel, to 0.1°C resolution. Aggregate temperatures are displayed in each voxel for luteal females ($n=14$) and males ($n=20$) separately. (B) Linear mixed modelling results for T_{Br} by time of day; results for global T_{Br} (left) and deep brain T_{Br} (thalamus and hypothalamus, right) are shown. Solid red lines represent model fits, shaded areas represent 95% confidence intervals, dark grey circles display residuals (single temperature data points), and smoothed dashed yellow lines represent partial residuals. The x-axis for Time summarizes the continuous variable of time distance since the participant's MSF_{sc} (proportion of a linearized unit circle, where $0=MSF_{sc}$ and $1=24$ hours). (C) Temperature range (maximum versus minimum across three tested time points) for oral and hypothalamic sites for each

healthy participant (n=39). Temperature varied more by time of day in the hypothalamus than orally (repeated measures one-way ANOVA with Sidak's multiple comparisons test ****P<0.0001; see fig.S6B for other brain regions). **(D)** 24-hour temperature rhythms of the healthy brain, double plotted. Interpolated average T_{Br} rhythms in healthy luteal females (n=14) and males (n=20) based on sinusoidal fit using temperatures measured at three time points. Note higher temperatures in all regions in luteal females relative to males and marked variation in deep brain temperatures in males. Arrows point to predicted T_{Br} minima around 2–3am (approaching MSF_{sc}). Sup1–4, superficial brain regions 1–4 from medial to lateral; Hypo, hypothalamus; Thal, thalamus.

HEATWAVE—a 4D map of human brain temperature

Combining our spatial and temporal observations, we built HEATWAVE—a 4-dimensional map to model human T_{Br} at hourly resolution (Movies S1 and S2). HEATWAVE can be dynamically explored at (<https://www2.mrc-lmb.cam.ac.uk/groups/oneill/research/heatwave/>). These comparisons highlight the relatively hot deep brain regions and their greater diurnal variation in males than females. The HEATWAVE videos complement the voxel maps in Fig.3A, which represent a reference resource for interpreting human T_{Br} at each of the time points tested. Since each data point in each map is an average of data from multiple individuals, it incorporates the range of ages, BMIs, and chronotypes expected for each sex in the demographic tested. Our data collection points also cater for the times (morning and afternoon) when most patients would present for MR-based neuroimaging in the non-acute setting. In addition to modelling diurnal human T_{Br} in a continuous fashion, HEATWAVE thus provides the first comprehensive spatially-resolved description of normal human T_{Br} at three clinically-relevant time points; a rich reference dataset for future studies in different age groups and patient cohorts.

Daily brain temperature rhythms predict patient survival

The characterisation of physiological T_{Br} variation in humans allows its dysregulation by brain injury to be understood in context for the first time. Of 134 eligible patient records screened, 114 had at least 24h of temperature data recorded (criteria level A). Of these, 110 patients had sufficient temperature data (≥ 36 h) for diurnal rhythm analysis (criteria levels A and B; for eight of these patients, sufficient data was available for T_{Bo} only). Outcome in intensive care was available for 113/114 patients (criteria levels A and C), and a complete set of injury severity scores (PLR, GCS, and GCSM) was available for 109/114 patients (criteria levels A, C, D). A total of 107 patients met all criteria levels, and 100 patients had sufficient data to test for an association between diurnal T_{Br} rhythmicity and outcome (mortality). Summary data are shown in Table 3. As in our healthy cohort, mean T_{Br} (38.5 SD 0.8°C) was significantly higher than mean T_{Bo} (37.5 SD 0.5°C; $P < 0.0001$, Fig.4A), but the range was much wider (32.6 to 42.3°C). T_{Br} was not affected by the site of intracranial probe placement relative to focal injury (fig.S7). We found an approximately daily temperature rhythm in 25/110 patients, of which 23 had a daily T_{Br} rhythm (Fig.4B, fig.S8). However, across the cohort, the timings of temperature maxima and minima were poorly aligned with the external day-night cycle. This desynchronization of internal timing from the external solar cycle is a hallmark of circadian rhythms when external timing cues are diminished,⁴¹ and lies in stark contrast to rectal temperature data from healthy individuals maintained in the presence of daily light/dark and feed/fast cues (Fig.4C).

	Females	Males
Age (y)	55.1 (14.8) n=21	45.7 (17.2) n=94
T_{Br} Mean (°C)	38.2 (0.85) n=20	38.6 (0.85) n=85
T_{Bo} Mean (°C)	37.2 (0.52) n=17	37.5 (0.51) n=78
T_{Br} Range (°C)	3.38 (1.21) n=20	3.21 (1.08) n=85
T_{Bo} Range (°C)	2.65 (0.93) n=17	2.50 (0.87) n=85
T_{Br} Max (°C)	39.8 (1.00) n=20	40.3 (1.03) n=85
T_{Bo} Max (°C)	38.4 (0.70) n=17	38.8 (0.71) n=85
T_{Br} Min (°C)	36.4 (1.07) n=20	37.1 (0.99) n=85
T_{Bo} Min (°C)	35.7 (0.82) n=17	36.3 (0.76) n=85
PLR	1.86 (0.36) n=21	1.77 (0.59) n=86
GCS	7.90 (3.42) n=21	8.07 (3.60) n=87
GCSM	4.10 (1.61) n=21	3.71 (1.85) n=87

Table 3. TBI patient demographics and summary temperature data. Data presented as mean (SD); Min, minimum; Max, maximum; PLR, presence of pupillary light reflex in one or both eyes; GCS, Glasgow Coma Score; GCSM, Glasgow Coma Score Motor response. Individual patient temperature values and ranges were calculated from all available data present within the data analysis window that met inclusion/exclusion criteria (Table 1); aggregate results for males and females are presented here.

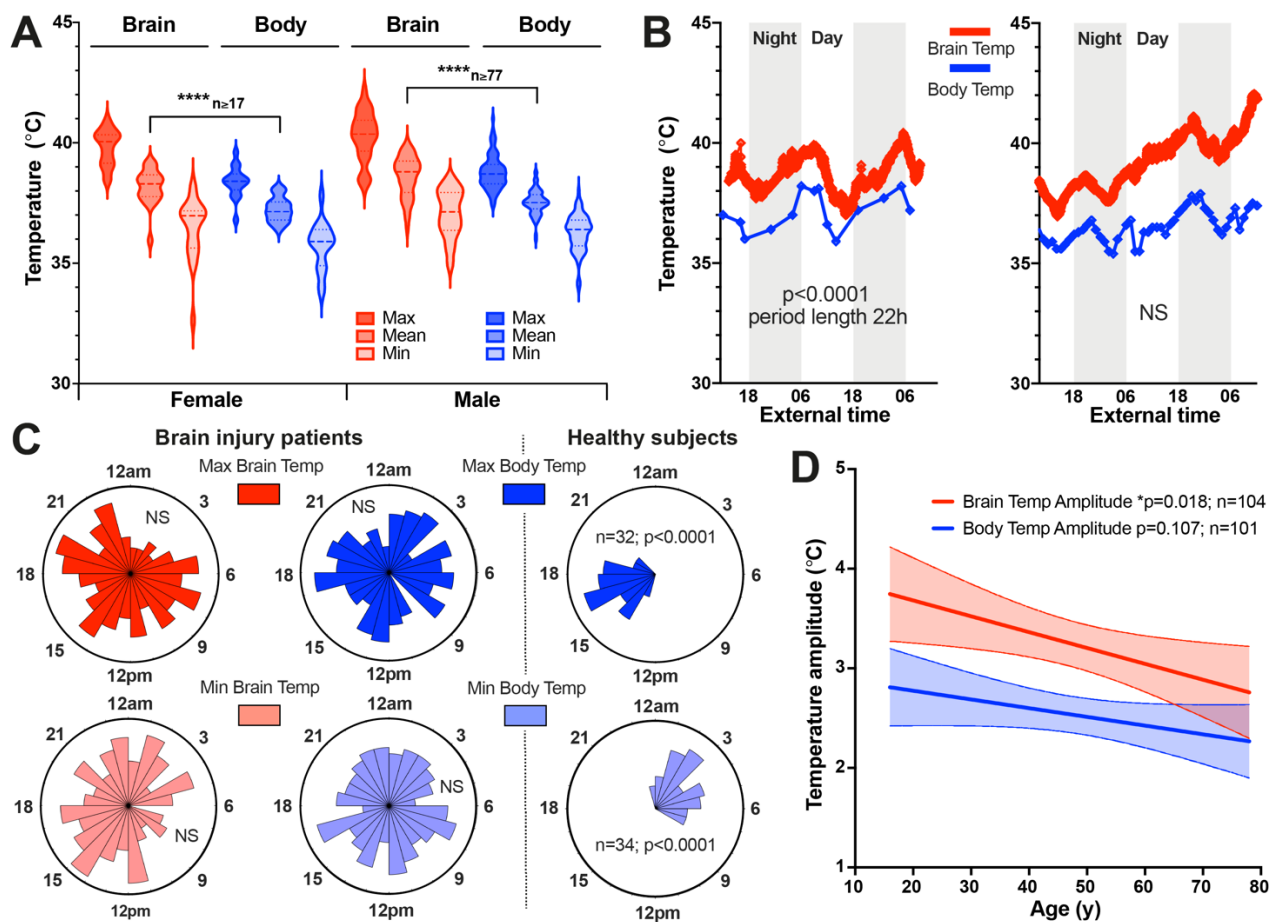


Fig. 4. Temperature rhythms in TBI patients. (A) Violin plot of patient T_{Br} and T_{Bo} according to sex. Mean T_{Br} significantly greater than mean T_{Bo} , mixed effects analysis with Tukey's for multiple comparisons (**** $P < 0.0001$, females, $n = 20$ for T_{Br} and $n = 17$ for T_{Bo} ; males, $n = 85$ for T_{Br} and $n = 77$ for T_{Bo}). (B) Representative raw data from 62 y female patient (left) showing daily variation in T_{Br} and T_{Bo} , with T_{Br} consistently higher than T_{Bo} and both parameters in same phase. T_{Br} sampled once per minute; peak at 05:28 and nadir at 16:12 highlighting inversion of phase relationship with external day-night cycle under intensive care conditions (external time in 24-hour clock format). Representative raw data from 42 y male patient (right) showing lack of a daily rhythm in both T_{Br} and T_{Bo} . (C) Rose plots (left) showing timings of temperature maxima and minima in 114 TBI patients (24-hour clock format). For all variables, the null hypothesis of a uniform distribution could not be rejected (Rayleigh test of uniformity; $T_{Br}Max$, $n = 104$, $P = 0.20$; $T_{Br}Min$, $n = 104$, $P = 0.16$; $T_{Bo}Max$, $n = 101$, $P = 0.99$; $T_{Bo}Min$, $n = 101$, $P = 0.86$). Contrast with healthy subject rectal temperature

data from publicly-available database (right).⁴² **(D)** Linear regression of patient temperature ranges with age; reduction in temperature amplitude significant for brain (slope of -0.016 significantly different from zero; 95% confidence interval -0.029 to 0.003). Shaded areas represent 95% confidence intervals for lines of best fit. Max, maximum; Min, minimum; NS, not significant.

As for healthy adults, there was a relationship between T_{Br} and age; T_{Br} amplitude was reduced in older patients ($P=0.018$), dominated by an upward trend in minimum temperature (Fig.4D, fig.S9). Twenty-five patients died in intensive care. Applying a GLMM (Fig.5), we found that lack of a daily T_{Br} rhythm, or an age increase of 10 years, increased the odds of death in intensive care 12-fold and 11-fold, respectively (OR for death with rhythm 0.09; 95% confidence interval 0.01 to 0.84, $P=0.035$ and OR for death with ageing by 1 year 1.10; 1.05 to 1.16, $P=0.0002$). These relationships could not be explained by a general elevation in T_{Br} , since mean T_{Br} was positively associated with survival (OR for death 0.45 for 1°C increase, 0.21 to 0.96, $P=0.040$). The presence of a diurnal T_{Br} rhythm did not correlate with either age or mean T_{Br} (Appendix 5). Together, these data show that daily temperature variation is frequently disrupted or absent in TBI patients and that T_{Br} variation is of greater prognostic use than absolute T_{Br} . Older TBI patients lacking a daily T_{Br} rhythm are at greatest risk of death in intensive care, and presence of a daily T_{Br} rhythm appears to be the strongest single predictor of survival after TBI.⁴³

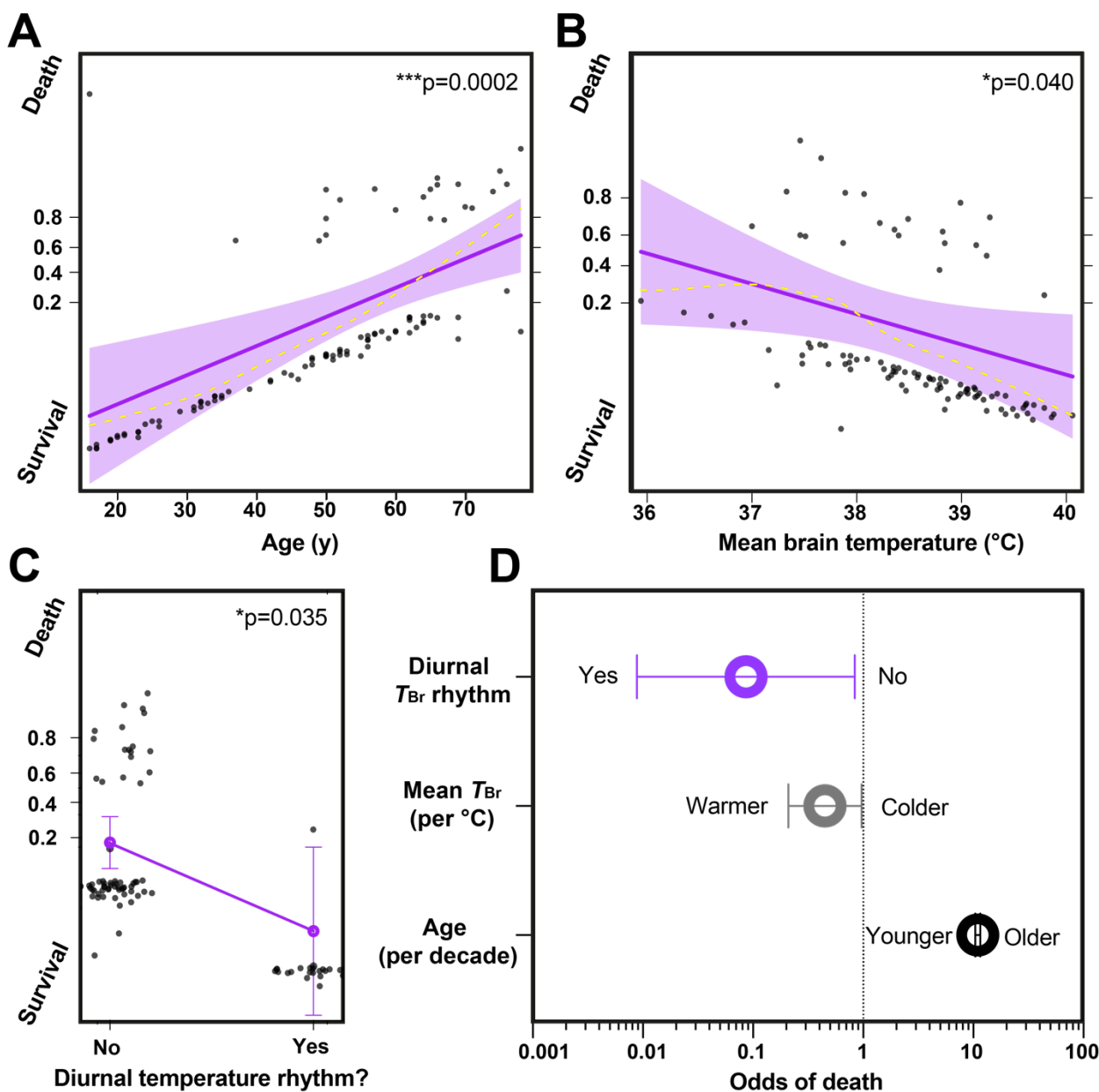


Fig. 5. A daily T_{Br} rhythm predicts survival after brain injury. (A-C) GLMM results for outcome in $n=100$ TBI patients. Probability of death (‘success’ or ‘hit’ = 1) relative to survival (‘failure’ or ‘miss’ = 0) is depicted on the y-axis. Solid purple lines represent model fits for logit (log of the odds) binomial distribution for a given predictor and dark grey circles display residuals (individual patients). For numerical predictors (A-B), shaded areas represent 95% confidence intervals and smoothed dashed yellow lines represent partial residuals. For the categorical predictor of presence/absence of diurnal temperature rhythm (C), residuals are jittered in the x-axis direction for visibility and 95% confidence intervals are presented as double-ended error bars. (D) Odds of death

in intensive care transformed from the data in (A-C); the results for these three predictors are significant since the 95% confidence intervals (double-ended error bars) do not include 1. Note also that confidence intervals become numerically asymmetric once transformed from log odds to regular odds. Only factors that demonstrated a statistically significant relationship with mortality are shown. Note logarithmic scale on x-axis and large effect size for presence of a daily rhythm in T_{Br} in (D). See Methods and Supplementary Methods for further details on the GLMM, and Appendix 5 for all numerical outputs and related code.

DISCUSSION

Principal findings

We have established a 4-dimensional map of human T_{Br} , and shown how this parameter varies with time of day, brain region, age, and sex in healthy adults. These data provide clinicians with an urgently-needed and readily-accessible reference resource for evidence-based interpretation of T_{Br} data in patients. Furthermore, we have found a relationship between the presence of a daily T_{Br} rhythm and survival of TBI patients. Our findings demonstrate the high prognostic value of time-resolved T_{Br} measurements in neurocritical care, thus empowering a temperature-based prediction of mortality.²² Overall, this work reveals marked heterogeneity and dynamism of human T_{Br} that must influence neural cell activity, and represents an important correlate of brain health.

Strengths and limitations

Although time-based human neuroimaging studies are sparse, some morning/afternoon comparisons are consistent with diurnal regulation of brain morphometry,^{44,45} as well as diurnal variation in neural activity and metabolism.⁴⁶⁻⁴⁸ However, prior studies were underpowered without consideration of chronotype and a late evening time point, which provides greater insight into healthy brain

physiology by incorporating the period approaching habitual sleep time (Fig.3). It was neither practical nor clinically-relevant to deprive our participants of all external timing cues (to derive circadian T_{Br} variation), but this diurnal T_{Br} variation is almost identical to direct measurements obtained in healthy non-human primates under stringent conditions.¹⁸ Though unlikely, it is conceivable that gross regional differences in the activity of cellular water impact upon the apparent spatial T_{Br} variation we observe within an individual at a given time point. However, we are unaware of any supporting evidence for this, nor can it be attributed to simple grey versus white matter distribution.⁴⁹ Moreover, such differences cannot influence the T_{Br} variation we have found in relation to time of day, sex, age, or menstrual cycle stage. This is illustrated well when we limit our model to a subset of deep brain regions of more homogenous tissue structure, where T_{Br} variation persists with respect to all of the aforementioned fixed effects (Fig.2B, 3B, fig.S6). Crucially, our robust statistical approach caters for multiple physiologically-relevant confounders within and between individuals that would have prevented the detection of significant T_{Br} variation in previous studies.^{49,50} Alongside the patient data (Fig.5), and multiple parallel methods of temperature measurement in healthy subjects by us and others,^{22,51-53} our results offer compelling evidence of a daily temperature rhythm throughout the normal human brain (Supplementary Text '*Temperature rhythms and sleep*').

The within-brain temperature gradient is remarkable (Fig.2B). As an 'open' thermodynamic system performing no mechanical work, aerobic metabolism of the brain releases heat at ~ 0.66 J/min/g of tissue which is primarily removed by CBF.^{38,54-56} It is therefore highly likely that regional variation in neurovascular anatomy plays the chief role in creating spatial T_{Br} gradients (Supplementary Text '*Temperature gradients*'). Although we cannot completely exclude a contribution from regional differences in water content,^{49,57} these are unlikely to explain the temperature difference between the thalamus and hypothalamus (both grey matter structures devoid of cerebrospinal fluid). We suggest

that the lower temperature of the hypothalamus might reflect its closer proximity to major vascular networks such as the Circle of Willis. In principle, technical limitations (Supplementary Text ‘*Technical limitations of brain thermometry*’) could potentially exaggerate MRS-derived temperature differences at the extreme edges of regions of interest (cerebral layer Sup4). The spatial distribution we have found is however very similar to non-human primates, excepting a larger gradient magnitude that is entirely consistent with the difference in brain volume between humans and rhesus monkeys.¹⁹ Unlike previous studies,^{49,50} we make no baseline assumption that temperature should be homogeneous across brain regions, nor between different tissue types within the brain. Importantly, we did not apply a post-acquisition correction to our MRS data to equalize temperatures between grey and white matter,^{49,50} since this would perpetuate the above assumption, and overlooks the clear tissue temperature differences observed in non-human primates and normothermic human patient brains.^{14,16,19} Indeed, higher temperatures in white matter-rich areas concur with predictions based on modelling perfusion, blood volume fraction, and heat generation in different brain tissues.^{13,58-60}

Possible mechanisms and implications

An increase in mean T_{Br} (Fig.2B) and a trend upwards in minimum T_{Br} (fig.S9) with age suggests that overnight brain cooling becomes less efficient in older people, leading to a damped T_{Br} rhythm. This age-dependent reduction in T_{Br} amplitude is consistent with studies of T_{Bo} and may contribute to the disrupted sleep patterns and ‘sundowning’ symptoms of dementia patients.^{24,61-63} Cerebral blood supply is considered so efficient that heat removal is achieved without the need for other mechanisms under most circumstances,^{36,37,64} which seems intuitive for the young, healthy brain. However, the vast literature linking neurodegeneration to cerebrovascular compromise indicates that our key brain cooling mechanism progressively deteriorates with age (Supplementary Text ‘*Internal rhythms and health*’).^{65,66} Neuronal activity is highly sensitive to temperature change, with a Q_{10} of ~ 2.3 , although this is generally considered to be most problematic in the acute setting.^{38,55,67} In a

study of 1130 epilepsy patients, 80–92% showed a 24-hour cycle of seizure rates, with events most common at ~8am, when T_{Br} should increase most steeply (Fig.3D).⁶⁸ Given that cooling can terminate epileptic discharges,⁶⁹ diurnal changes in T_{Br} may well contribute to diurnal variation in the incidence of seizures and cluster headache.^{70,71}

T_{Bo} increases, and its overnight drop is blunted, in luteal versus follicular phase women.^{52,72} This menstrual variation predicts that T_{Bo} is ~0.4°C higher in the early luteal phase.⁷² For the first time, we report a parallel luteal-phase increase in global T_{Br} by ~0.36°C, and of deep T_{Br} by 0.82°C (95% confidence interval 0.37 to 1.28, P=0.0006). This may contribute to the reported variable sleep patterns and changes in cognition across different stages of the menstrual cycle.^{52,73} A thermogenic effect of progesterone is well-recognized, and may involve direct stimulation of preoptic/anterior hypothalamic thermoregulatory neurons, or the suprachiasmatic nucleus.^{52,53,74,75} Despite its postulated neuroprotective effects, large clinical trials have failed to show any benefit of progesterone therapy for TBI—one reason for this could be damping of the daily T_{Br} rhythm (Fig.3D).⁷⁶ It is widely accepted that BMI positively correlates with T_{Bo} as found here (Fig.1).^{22,77} Since BMI was slightly higher in males relative to females in our healthy cohort, a difference in BMI cannot explain the higher T_{Br} observed in luteal females and, notably, there was no relationship between BMI and T_{Br} overall (Fig.2B; Appendix 5). This supports our conclusion that T_{Br} cannot be solely dependent on, nor predicted from, T_{Bo} since brain heat removal also occurs through routes that are unaffected by adipose deposition.^{36,37}

Essential to clinical diagnostics is the comparison of patient data with reference ranges from healthy individuals; MRS-thermometry now makes this possible for T_{Br} . We have validated our core MRS findings using multiple complementary methods of temperature measurement. This is most pressing for T_{Br} , where such methods are effectively mutually exclusive in healthy individuals and

neurocritical care patients. TTM is the mainstay of neuroprotection subsequent to out-of-hospital cardiac arrest.⁷⁸ Here, the objective is to reduce T_{Br} , which is rarely measured directly in trials that test the therapeutic value of TTM in the context of brain injury. Cooling adults at the ‘wrong’ biological time or fixing patient temperatures at a constant target value may further compromise thermoregulation by abolishing physiologically-important, health-critical temperature variation. The highest temperature we observed in any healthy individual was 40.9°C in the thalamus of a luteal female in the afternoon; whilst the perception exists that a T_{Br} of this value would cause brain damage, there is no direct evidence for this, and similar deep brain temperatures are observed physiologically in other mammalian species.⁷⁹ Furthermore, the T_{Br} range in our volunteers raises doubt over whether T_{Br} was abnormally high in some patient reports.¹⁵ Current temperature management guidelines do not consider physiological differences by sex or time of day,⁸⁰ and whether adults should be cooled at all in neurocritical care remains controversial. A clear understanding of how and why T_{Br} varies in health and disease is thus imperative. Here we report a healthy cortical white matter maximum T_{Br} of 40.3°C, but we caution strongly against overinterpreting single T_{Br} values or transitory trends. Rather, we recognize the need for technological solutions that allow individualized target temperature ranges to be determined, facilitating decision making that incorporates chronotype, age, sex, menstrual cycle, and time of day.

Unanswered questions and future research

Prospective controlled trials are needed to confirm the predictive power of T_{Br} rhythmicity in relation to patient outcome, as well as the clinical utility of TTM protocols in brain-injured patients. There may be high clinical value in exploiting T_{Br} variation to detect or monitor focal pathologic processes such as neoplasia, trauma, vascular insults, and epileptogenesis, but also more distributed inflammatory, metabolic, and neuropsychiatric diseases.^{54,81-87} In particular, future work should be directed to address whether abnormal T_{Br} rhythmicity may serve as an early biomarker of

neurodegeneration; a mechanistically opaque process for which early diagnostics are notably deficient.^{26,65} Beyond brain injury and disease (Supplementary Text ‘*Clinical applications*’), our results further question the value of single-point temperature measurements using peripheral thermometers.⁸⁸ We have shown that more sophisticated analyses can better exploit temperature as a clinical tool. Wearable devices now permit easy and convenient recording of daily rhythms in many physiological parameters. Algorithm-based temperature profiling will help accomplish the goals of precision medicine, not just for individuals,⁸⁹ but at scale. For example, in an infectious disease outbreak, real-time screening for fever development could rapidly identify high-risk individuals by deviation from their own temperature rhythm, rather than a population ‘mean’ or by random testing. Personalized, digital, round-the-clock temperature monitoring would thus advance remote health tracking and evidence-based enforcement of global health policy in the context of emerging disease. Whilst providing excellent spatial resolution, MRS brain thermometry is clearly impractical for routine use in most clinical settings. Since core T_{Bo} is not a faithful proxy for T_{Br} ,⁹⁰ our work highlights an urgent need for cost-effective, non-invasive technologies that can capture longitudinal variations in T_{Br} , alongside core body and peripheral temperatures.

REFERENCES

- 1 Grodzinsky E, Levander MS. History of the thermometer. *Understanding Fever and Body Temperature* 2019;23-25. doi: 10.1007/978-3-030-21886-7_3
- 2 Phillips MA, Burrows JN, Manyando C, Hooft van Huijsduijnen R, Van Voorhis WC, Wells TNC. Malaria. *Nat Rev Dis Primers* 2017;3:17050
- 3 Busto R, Dietrich WD, Globus MY, Valdes I, Scheinberg P, Ginsberg MD. Small differences in intraschemic brain temperature critically determine the extent of ischemic neuronal injury. *J Cereb Blood Flow Metab* 1987;7:729-738

- 4 Childs C, Vail A, Protheroe R, King AT, Dark PM. Differences between brain and rectal temperatures during routine critical care of patients with severe traumatic brain injury. *Anaesthesia* 2005;60:759-765
- 5 Abu-Arafeh A, Rodriguez A, Paterson RL, Andrews PJD. Temperature variability in a modern targeted temperature management trial. *Crit Care Med* 2018;46:223-228
- 6 Dehkhargani S, Fleischer CC, Qiu D, Yepes M, Tong F. Cerebral temperature dysregulation: MR thermographic monitoring in a nonhuman primate study of acute ischemic stroke. *AJNR Am J Neuroradiol* 2017;38:712-720
- 7 Rumana CS, Gopinath SP, Uzara M, Valadka AB, Robertson CS. Brain temperature exceeds systemic temperature in head-injured patients. *Crit Care Med* 1998;26:562-567
- 8 Karaszewski B, Wardlaw JM, Marshall I et al. Early brain temperature elevation and anaerobic metabolism in human acute ischaemic stroke. *Brain* 2009;132:955-964
- 9 Karaszewski B, Carpenter TK, Thomas RGR et al. Relationships between brain and body temperature, clinical and imaging outcomes after ischemic stroke. *J Cereb Blood Flow Metab* 2013;33:1083-1089
- 10 Moser E, Mathiesen I, Andersen P. Association between brain temperature and dentate field potentials in exploring and swimming rats. *Science* 1993;259:1324-1326
- 11 Henker RA, Brown SD, Marion SW. Comparison of brain temperature with bladder and rectal temperatures in adults with severe head injury. *Neurosurgery* 1998;42:1071-1075
- 12 Rossi S, Zanier ER, Mauri I, Columbo A, Stocchetti N. Brain temperature, body core temperature, and intracranial pressure in acute cerebral damage. *J Neurol Neurosurg Psychiatry* 2001;71:448-454
- 13 Thrippleton MJ, Parikh J, Harris B et al. Reliability of MRSI brain temperature mapping at 1.5 and 3 T. *NMR Biomed* 2014;27:183-90
- 14 Mariak Z. Intracranial temperature recordings in human subjects. The contribution of the

- neurosurgeon to thermal physiology. *J Therm Biol* 2002; 27:219-228.
[https://doi.org/10.1016/S0306-4565\(01\)00087-0](https://doi.org/10.1016/S0306-4565(01)00087-0)
- 15 Mellergård P. Changes in human intracerebral temperature in response to different methods of brain cooling. *Neurosurgery* 1992;31:671-677.
 - 16 Mellergård P. Monitoring of rectal, epidural, and intraventricular temperature in neurosurgical patients. *Acta Neurochir. Suppl. (Wien)* 1994;60:485-487
 - 17 Shiraki K, Sagawa S, Tajima F, Yokota A, Hashimoto M, Brengelmann GL. Independence of brain and tympanic temperatures in an unanaesthetised human. *J Appl Physiol (1985)* 1988;65:482-486
 - 18 Maloney SK, Mitchell D, Mitchell G, Fuller A. Absence of selective brain cooling in unrestrained baboons exposed to heat. *Am J Physiol Regul Integr Comp Physiol* 2007;292: R2059-2067
 - 19 Hayward JN, Baker MA. Role of cerebral arterial blood in the regulation of brain temperature in the monkey. *Am J Physiol* 1968;215:389-403
 - 20 Hastings MH, O'Neill JS, Maywood ES. Circadian clocks: regulators of endocrine and metabolic rhythms. *J Endocrinol* 2007;195:187-98
 - 21 Conroy DA, Spielman AJ, Scott RQ. Daily rhythm of cerebral blood flow velocity. *J Circadian Rhythms* 2005;3:3. doi:10.1186/1740-3391-3-3
 - 22 Obermeyer Z, Samra JK, Mullainathan S. Individual differences in normal body temperature: longitudinal big data analysis of patient records. *BMJ* 2017;359:j5468. doi: 10.1136/bmj.j5468
 - 23 Morris Z, Whiteley WN, Longstreth et al. Incidental findings on brain magnetic resonance imaging: systematic review and meta-analysis. *BMJ* 2009;339:b3016
 - 24 Logan RW, McClung CA. Rhythms of life: circadian disruption and brain disorders across the lifespan. *Nat Rev Neurosci* 2019;20:49-65

- 25 Takahashi JS. Transcriptional architecture of the mammalian circadian clock. *Nat Rev Genet* 2017;18:164-179
- 26 Kondratova AA, Kondratov RV. The circadian clock and pathology of the ageing brain. *Nat Rev Neurosci* 2012;13:325-335
- 27 Roenneberg T, Merrow M. The circadian clock and human health. *Curr Biol* 2016; 26:R432-443
- 28 Roenneberg T, Pilz LK, Zerbini G, Winnebeck EC. Chronotype and Social Jetlag: A (Self-) Critical Review. *Biology* 2019;8:54. doi:10.3390/biology8030054
- 29 Cady EB, D'Souza PC, Penrice J, Lorek A. The estimation of local brain temperature by in vivo 1H magnetic resonance spectroscopy. *Magn Reson Med* 1995;33:862-867
- 30 Carney N, Totten AM, O'Reilly C et al. Guidelines for the management of severe traumatic brain injury, Fourth Edition. *Neurosurgery* 2017;80:6-15
- 31 Zielinski T, Moore AM, Troup E, Halliday KJ, Millar AJ. Strengths and limitations of period estimation methods for circadian data. *PLoS ONE* 2014;9:e96462
- 32 Lueck S, Thurley K, Thaben PF, Westermarck PO. Rhythmic degradation explains and unifies circadian transcriptome and proteome data. *Cell Rep* 2015;9:741-751
- 33 Babyak MA. What you see may not be what you get: a brief, non-technical introduction to overfitting in regression-type models. *Psychosom Med* 2004;66:411-421. doi: 10.1097/01.psy.0000127692.23278.a9
- 34 Erikson R. Oral temperature differences in relation to thermometer and technique. *Nurs Res* 1980;29:157-64
- 35 Ortiz-Tudela E, Martinez-Nicolas A, Campos M, Rol MA, Madrid JA. A new integrated variable based on thermometry, actimetry and body position (TAP) to evaluate circadian system status in humans. *PLoS Comput Biol* 2010;6:e1000996. doi:10.1371/journal.pcbi.1000996

- 36 Brengelmann GL. Specialised brain cooling in humans? *FASEB J* 1993;7:1148-1153
- 37 Cabanac M. Selective brain cooling in humans: “fancy” or fact? *FASEB J* 1993;7:1143-1147
- 38 Wang H, Wang B, Normoyle KP et al. Brain temperature and its fundamental properties: a review for clinicians and neuroscientists. *Front Neurosci* 2014;8:307.
doi:10.3389/fnins.2014.00307
- 39 Dunlap JC, Loros JJ, DeCoursey PJ. Chronobiology: biological timekeeping. Sinauer Associates, Sunderland, Mass, 2004
- 40 Baud MO, Magistretti PJ, Petit J-P. Sustained sleep fragmentation affects brain temperature, food intake, and glucose tolerance in mice. *J Sleep Res* 2013;22:3-12
- 41 Skene DJ, Skornyakov E, Chowdhury NR et al. Separation of circadian- and behaviour-driven metabolite rhythms in humans provides a window on peripheral oscillators and metabolism. *PNAS* 2018;115:7825-7830. <https://doi.org/10.1073/pnas.1801183115>
- 42 Kemp B, Zwinderman AH, Tuk B, Kamphuisen HAC, Obery JLL. Analysis of a sleep-dependent neuronal feedback loop: the slow-wave microcontinuity of the EEG. *IEEE-BME* 2000;47:1185-1194. Data set located at PhysioNet: Goldberger AL, Amaral LA, Glass et al. PhysioBank, PhysioToolkit, and PhysioNet: Components of a new research resource for complex physiological signals. *Circulation* 2000;101:pp.e215-e220
- 43 Steyerberg EW, Mushkudiani N, Perel P et al. Predicting outcome after traumatic brain injury: development and international validation of prognostic scores based on admission characteristics. *PLoS Med* 2008;5:e165. doi:10.1371/journal.pmed.0050165
- 44 Trefler A, Sadeghi N, Thomas AG, Pierpaoli C, Baker CI, Thomas C. Impact of time-of-day on brain morphometric measures derived from T1-weighted magnetic resonance imaging. *Neuroimage* 2016;133:41-52
- 45 Nakamura K, Brown RA, Narayanan S, Collins DL, Arnold DL. Alzheimer’s Disease Neuroimaging Initiative. Diurnal fluctuations in brain volume: statistical analyses of MRI

- from large populations. *Neuroimage* 2015;118:126-132
- 46 Jiang C, Yi L, Su S et al. Diurnal variations in neural activity of healthy human brain decoded with resting-state blood oxygen level dependent fMRI. *Front Hum Neurosci* 2016;10:634.
- 47 Arm J, Al-ledani O, Lea R, Lechner-Scott J, Ramadan S. Diurnal variability of metabolites in healthy human brain with 2D localized correlation spectroscopy (2D L-COSY). *J Magn Reson Imaging* 2019;50:592-601
- 48 Soreni N, Noseworthy MD, Cormier T, Oakden WK, Bells S, Schachar R. Intraindividual variability of striatal 1H-MRS brain metabolite measurements at 3 T. *Magn Reson Imaging* 2006;24:187-194
- 49 Maudsley AA, Goryawala MZ, Sheriff S. Effects of tissue susceptibility on brain temperature mapping. *Neuroimage* 2017;146:1093-1101
- 50 Chadzynski GL, Bender B, Groeger A, Erb M, Klose U. Tissue specific resonance frequencies of water and metabolites within the human brain. *J Magn Reson* 2011;212:55-63.
- 51 Aschoff VJ, Wever R. Spontanperiodik des menschen bei ausschluß aller zeitgeber. *Naturwissenschaften* 1962;49:337-342
- 52 Baker FC, Driver HS, Paiker J, Rogers GG, Mitchell D. Acetaminophen does not affect 24-h body temperature or sleep in the luteal phase of the menstrual cycle. *J Appl Physiol* (1985) 2002;92:1684-1691
- 53 Baker FC, Waner JI, Vieira EF, Taylor SR, Driver HS, Mitchell D. Sleep and 24 hour body temperatures: a comparison in young men, naturally cycling women and women taking hormonal contraceptives. *J Physiol* 2001;530:565-574
- 54 Yablonskiy DA, Ackerman JJ, Raichle ME. Coupling between changes in human brain temperature and oxidative metabolism during prolonged visual stimulation. *Proc Natl Acad Sci USA* 2000;97:7603-7608
- 55 Rango M, Arighi A, Bonifati C, Del Bo R, Comi G, Bresolin N. The brain is hypothermic in

- patients with mitochondrial diseases. *J Cereb Blood Flow Metab* 2014;34: 915-920
- 56 Kaupinnen RA, Vidyasagar R, Childs C, Balanos GM, Hiltunen Y. Assessment of human brain temperature by 1H MRS during visual stimulation and hypercapnia. *NMR Biomed* 2008;21:388-395
- 57 Birkl C, Langkammer C, Haybaeck J et al. Temperature dependency of T1 relaxation time in unfixed and fixed human brain tissue. *Biomed Tech (Berl)* 2013;58 Suppl 1.pii/j/bmte.2013.58.issue-s1-L/bmt-2013-4290/bmt-2013-4290.xml. doi: 10.1515/bmt-2013-4290
- 58 Blowers S, Marshall I, Thrippleton M, et al. How does blood regulate cerebral temperatures during hypothermia? *Sci Rep* 2018;8:7877.
- 59 Neimark MA, Konstas A-A, Choi J-H, Pile-Spellman J. Brain cooling maintenance with cooling cap following induction with intracarotid cold saline infusion: a quantitative model. *J Theor Biol* 2008;253:333-44. doi: 10.1016/j.jtbi.2008.03.025
- 60 Larsson HBW, Courivaud F, Rostrup E, Hansen AE. Measurement of brain perfusion, blood volume, and blood-brain barrier permeability, using dynamic contrast-enhanced T(1)-weighted MRI at 3 tesla. *Magn Reson Med* 2009;62:1270-81. doi:10.1002/mrm.22136
- 61 Czeisler CA, Dumont M, Duffy JF et al. Association of sleep-wake habits in older people with changes in output of circadian pacemaker. *Lancet* 1992;340:933-936
- 62 Ferrari E, Magri F, Locatelli M et al. Chrono-neuroendocrine markers of the aging brain. *Aging (Milano)* 1996;8:320-327
- 63 Sumida K, Sato N, Ota M et al. Intraventricular temperature measured by diffusion-weighted imaging compared with brain parenchymal temperature measured by MRS in vivo. *NMR Biomed* 2016;29:890-895
- 64 Simon E. Tympanic temperature is not suited to indicate selective brain cooling in humans: a re-evaluation of the thermophysiological basics. *Eur J Appl Physiol* 2007;101:19-30

- 65 Wardlaw JM, Smith EE, Biessels GJ et al. Standards for Reporting Vascular Changes on Neuroimaging (STRIVE v1). Neuroimaging standards for research into small vessel disease and its contribution to ageing and neurodegeneration. *Lancet Neurol* 2013;12:822-838
- 66 Nedergaard M, Goldman SA. Glymphatic failure as a final common pathway to dementia. *Science* 2020;370:50-56
- 67 Rango M, Bonifati C, Bresolin N. Post-activation brain warming: a thermometry study. *PLoS ONE* 2015;10:e0127314
- 68 Karoly PJ, Goldenholz DM, Freestone DR et al. Circadian and circaseptan rhythms in human epilepsy: a retrospective cohort study. *Lancet Neurol* 2018;17:977-985
- 69 Nomura S, Kida H, Hirayama Y et al. Reduction of spike generation frequency by cooling in brain slices from rats and from patients with epilepsy. *J Cereb Blood Flow Metab* 2019;39:2286-2294
- 70 May A, Bahra A, Büchel C, Frackowiak RS, Goadsby PJ. Hypothalamic activation in cluster headache attacks. *Lancet* 1998;352:275-278
- 71 Lodi R, Pierangeli G, Tonon C et al. Study of hypothalamic metabolism in cluster headache by proton MR spectroscopy. *Neurology* 2006;66:1264-1266
- 72 Baker FC, Driver HS, Rogers GG, Paiker J, Mitchell D. High nocturnal body temperatures and disturbed sleep in women with primary dysmenorrhea. *Am J Physiol* 1999;277:E1013–E1021
- 73 Grant LK, Gooley JJ, St Hilaire MA et al. Menstrual phase-dependent differences in neurobehavioural performance: the role of temperature and the progesterone/estradiol ratio. *Sleep* 2020;43:zsz227. doi: 10.1093/sleep/zsz227
- 74 Nakayama T, Suzuki M, Ishizuka N. Action of progesterone on preoptic thermosensitive neurons. *Nature* 1975;258:80
- 75 Kruijver FP, Swaab DF. Sex hormone receptors are present in the human suprachiasmatic

- nucleus. *Neuroendocrinology* 2002;75:296-305
- 76 Ma J, Huang S, Qin S, You C, Zeng Y. Progesterone for acute traumatic brain injury. *Cochrane Database Syst Rev* 2016;12:CD008409
- 77 Geneva II, Cuzzo B, Fazili T, Javaid W. Normal body temperature: a systematic review. *Open Forum Infect Dis* 2019;6:ofz032. doi: 10.1093/ofid/ofz032
- 78 Hassager C, Nagao K, Hildick-Smith D. Out-of-hospital cardiac arrest: in-hospital intervention strategies. *Lancet* 2018;391:989-998
- 79 Fuller A, Carter RN, Mitchell D. Brain and abdominal temperatures at fatigue in rats exercising in the heat. *J Appl Physiol* 1998;84:877-883. doi: 10.1152/jappl.1998.84.3.877
- 80 Cariou A, Payen J-F, Asehnoune K et al. Targeted temperature management in the ICU: Guidelines from a French expert panel. *Anaesth Crit Care Pain Med* 2018;37:481-491.
- 81 Madden LK, Hill M, May TL et al. The implementation of targeted temperature management: an evidence-based guideline from the Neurocritical Care Society. *Neurocrit Care* 2017;27:468-487
- 82 Nanba T, Nishimoto H, Yoshioka Y et al. Apparent brain temperature imaging with multi-voxel proton magnetic resonance spectroscopy compared with cerebral blood flow and metabolism imaging on positron emission tomography in patients with unilateral chronic major artery steno-occlusive disease. *Neuroradiology* 2017;59:923-935
- 83 Tsutsui S, Nanba T, Yoshioka Y et al. Preoperative brain temperature imaging on proton magnetic resonance spectroscopy predicts hemispheric ischemia during carotid endarterectomy for unilateral carotid stenosis with inadequate collateral blood flow. *Neurol Res* 2018;40:617-623
- 84 Marshall I, Karaszewski B, Wardlaw JM et al. Measurement of regional brain temperature using proton spectroscopic imaging: validation and application to acute ischemic stroke. *Magn Reson Imaging* 2006;24:699-706

- 85 Sone D, Ikegaya N, Takahashi A et al. Noninvasive detection of focal brain hyperthermia related to continuous epileptic activities using proton MR spectroscopy. *Epilepsy Res* 2017; 138:1-4
- 86 Shiloh R, Kushnir T, Gilat Y et al. In vivo occipital-frontal temperature-gradient in schizophrenia patients and its possible association with psychopathology: a magnetic resonance spectroscopy study. *Eur Neuropsychopharmacol* 2008;18:557-564.
- 87 Nikitopoulou G, Crammer JL. Change in diurnal temperature rhythm in manic-depressive illness. *BMJ* 1976;1:1311-1314
- 88 Niven DJ, Gaudet JE, Laupland KB, Mrklas KJ, Roberts DJ, Stelfox HT et al. Accuracy of peripheral thermometers for estimating temperature: a systematic review and meta-analysis. *Ann Intern Med* 2015;163:768-777
- 89 Papaionnou VE, Chouvarda IG, Maglaveras NK, Pneumatikos IA. Temperature variability analysis using wavelets and multiscale entropy in patients with systemic inflammatory response syndrome, sepsis, and septic shock. *Crit Care Lond Engl* 2012;16:R51
- 90 Childs C, Lunn KW. Clinical review: brain-body temperature differences in adults with severe traumatic brain injury. *Critical Care* 2013;17:222.
<http://ccforum.com/content/17/2/222>

Acknowledgements:

We gratefully acknowledge CiBraT Study Radiographers at the Edinburgh Imaging (Royal Infirmary of Edinburgh) Facility (Gayle Barclay, Annette Cooper, Lucy Kessler, Donna McIntyre, Isla Mitchell, and Maddy Murphy) and CiBraT Study Participants; administrative support from Dawn Cardy, Joanne Douglas, and Duncan Martin; data management support from Dominic Job and Aidan Hutchison; governance support from the Academic and Clinical Central Office for Research and Development (ACCORD); recruitment support from Edinburgh Imaging, Edinburgh Neuroscience,

and the Centre for Clinical Brain Sciences; graphics support from Lesley McKeane and Matthew Fry (MRC Laboratory of Molecular Biology Visual Aids); writing support from Ramanujan Hegde (MRC Laboratory of Molecular Biology), and valuable discussion from Rachel Edgar (Imperial College London) and O'Neill Lab members. CENTER-TBI data extraction was supported by Erta Beqiri, University of Milan.

Contributors: NMR conceived the idea for the work, designed and orchestrated the study, conducted recruitment and data collection for the prospective study, analyzed and interpreted all data, prepared all tables and figures, and wrote and revised the manuscript. JSON made conceptual contributions to the prospective study and contributions to the overall study design, interpreted data, contributed to figure preparation, and revised the manuscript. IM and MJT collected, analyzed, and interpreted spectroscopy data, contributed to figure preparation, and revised the manuscript. FMC contributed to study design, devised the statistical analysis plan for the prospective study, and revised the manuscript. AE and MC contributed to study design, CENTER-TBI High Resolution ICU data curation and extraction, statistical analysis, and revised the manuscript. GM analyzed, interpreted, and reported on prospective structural MRI data, and revised the manuscript. JR collected and developed extraction methods for retrospective patient data, contributed to data analysis, and revised the manuscript. All authors contributed to the literature search. JR, IM, and JSON contributed equally to this work (are joint last authors). NMR and JSON are guarantors and joint corresponding authors; NMR and JSON both attest that all listed authors meet authorship criteria and that no others meeting the criteria have been omitted. Investigators for The CENTER-TBI High HR ICU Sub-Study include: Audny Anke, Department of Physical Medicine and Rehabilitation, University hospital Northern Norway; Ronny Beer, Department of Neurology, Neurological Intensive Care Unit, Medical University of Innsbruck, Innsbruck, Austria; Bo-Michael Bellander, Department of Neurosurgery & Anesthesia & intensive care medicine, Karolinska University Hospital, Stockholm, Sweden; Andras Buki, Department of Neurosurgery, University of

Pecs and MTA-PTE Clinical Neuroscience MR Research Group and Janos Szentagothai Research Centre, University of Pecs, Hungarian Brain Research Program, Pecs, Hungary; Giorgio Chevallard, NeuroIntensive Care, Niguarda Hospital, Milan, Italy; Arturo Chierigato, NeuroIntensive Care, Niguarda Hospital, Milan, Italy; Giuseppe Citerio, NeuroIntensive Care Unit, Department of Anesthesia & Intensive Care, ASST di Monza, Monza, Italy; and School of Medicine and Surgery, Università Milano Bicocca, Milano, Italy; Endre Czeiter, Department of Neurosurgery, University of Pecs and MTA-PTE Clinical Neuroscience MR Research Group and Janos Szentagothai Research Centre, University of Pecs, Hungarian Brain Research Program (Grant No. KTIA 13 NAP-A-II/8), Pecs, Hungary; Bart Depreitere, Department of Neurosurgery, University Hospitals Leuven, Leuven, Belgium; George Eapen, Shirin Frisvold, Department of Anesthesiology and Intensive Care, University Hospital Northern Norway, Tromso, Norway; Raimund Helbok, Department of Neurology, Neurological Intensive Care Unit, Medical University of Innsbruck, Innsbruck, Austria; Stefan Jankowski, Neurointensive Care, Sheffield Teaching Hospitals NHS Foundation Trust, Sheffield, UK; Daniel Kondziella, Departments of Neurology, Clinical Neurophysiology and Neuroanesthesiology, Region Hovedstaden Rigshospitalet, Copenhagen, Denmark; Lars-Owe Koskinen, Department of Clinical Neuroscience, Neurosurgery, Umea University Hospital, Umea, Sweden; Geert Meyfroidt, Intensive Care Medicine, University Hospitals Leuven, Leuven, Belgium; Kirsten Moeller, Department Neuroanesthesiology, Region Hovedstaden Rigshospitalet, Copenhagen, Denmark; David Nelson, Department of Neurosurgery & Anesthesia & intensive care medicine, Karolinska University Hospital, Stockholm, Sweden; Anna Piippo-Karjalainen, Helsinki University Central Hospital, Helsinki, Finland; Andreea Radoi, Department of Neurosurgery, Vall d'Hebron University Hospital, Barcelona, Spain; Arminas Ragauskas, Department of Neurosurgery, Kaunas University of technology and Vilnius University, Vilnius, Lithuania; Rahul Raj, Helsinki University Central Hospital, Helsinki, Finland; Jonathan Rhodes, Department of Anaesthesia, Critical Care & Pain Medicine NHS Lothian & University of Edinburgh, Edinburgh, UK; Saulius

Rocka, Department of Neurosurgery, Kaunas University of technology and Vilnius University, Vilnius, Lithuania; Rolf Rossaint, Department of Anaesthesiology, University Hospital of Aachen, Aachen, Germany; Juan Sahuquillo, Department of Neurosurgery, Vall d’Hebron University Hospital, Barcelona, Spain; Oliver Sakowitz, Klinik für Neurochirurgie, Klinikum Ludwigsburg, Ludwigsburg, Germany; Department of Neurosurgery, University Hospital Heidelberg, Heidelberg, Germany; Ana Stevanovic, Department of Anaesthesiology, University Hospital of Aachen, Aachen, Germany; Nina Sundström, Department of Radiation Sciences, Biomedical Engineering, Umea University Hospital, Umea, Sweden; Riikka Takala, Perioperative Services, Intensive Care Medicine, and Pain Management, Turku University Central Hospital and University of Turku, Turku, Finland; Tomas Tamosuitis, Neuro-intensive Care Unit, Kaunas University of Health Sciences, Kaunas, Lithuania; Olli Tenovuo, Rehabilitation and Brain Trauma, Turku University Central Hospital and University of Turku, Turku, Finland; Peter Vajkoczy, Neurologie, Neurochirurgie und Psychiatrie, Charité–Universitätsmedizin Berlin, Berlin, Germany; Alessia Vargiolu, NeuroIntensive Care Unit, Department of Anesthesia & Intensive Care, ASST di Monza, Monza, Italy; Rimantas Vilcinis, Department of Neurosurgery, Kaunas University of Health Sciences, Kaunas, Lithuania; Stefan Wolf, Interdisciplinary Neuro Intensive Care Unit, Charité–Universitätsmedizin Berlin, Berlin, Germany; Alexander Younsi, Department of Neurosurgery, University Hospital Heidelberg, Heidelberg, Germany.

Funding: The prospective CiBraT Study was funded by a Medical Research Council Clinician Scientist Fellowship awarded to NMR (MR/S022023/1). JSON is supported by the Medical Research Council (MC_UP_1201/4). Some of the data contributing to the retrospective analysis were obtained in the context of CENTER-TBI, a large collaborative project (EC grant 602150) supported by the European Union’s 7th Framework program (FP7/2007-2013). Additional funding for patient data collection was obtained from the Hannelore Kohl Stiftung (Germany), from OneMind (USA) and from Integra LifeSciences Corporation (USA). MJT acknowledges funding from the NHS Lothian

Research and Development Office. This research was independent from funders. Funders had no role in the study design; in the collection, analysis, and interpretation of data; in the writing of the report; or in the decision to submit the article for publication.

Competing interests: all authors have completed the Unified Competing Interest form (available on request from the corresponding author) and declare: no support from any organisation for the submitted work; no financial relationships with any organisations that might have an interest in the submitted work in the previous three years, no other relationships or activities that could appear to have influenced the submitted work.

Ethical approval: The prospective study was co-sponsored by the University of Edinburgh and NHS Lothian (R&D Project Number 2019/0133). Ethics approval was obtained from the Academic and clinical office for research support (ACCORD) Medical Research Ethics Committee (AMREC; Study Number 18-HV-045). All participants provided written informed consent to participate. For TBI patient data analysis, approval was provided by NHS Scotland (14/SS/1086, R&D Department, University Hospitals Division NHS Lothian 2015/0171) for data collected at the Intensive Care Unit, Western General Hospital, Edinburgh, UK. For data extracted from other clinical sites via the CENTER-TBI database, the CENTER-TBI study was conducted in accordance with all relevant laws of the EU if directly applicable or of direct effect and all relevant laws of the country where the Recruiting sites were located, including but not limited to, the relevant privacy and data protection laws and regulations (the “Privacy Law”), the relevant laws and regulations on the use of human materials, and all relevant guidance relating to clinical studies from time to time in force including, but not limited to, the ICH Harmonised Tripartite Guideline for Good Clinical Practice (CPMP/ICH/135/95) (“ICH GCP”) and the World Medical Association Declaration of Helsinki entitled “Ethical Principles for Medical Research Involving Human Subjects”. Informed Consent by the patients and/or the legal representative/next of kin was obtained, accordingly to the local legislations, for all patients recruited in the Core Dataset of CENTER-TBI and documented in the e-

CRF. Ethical approval was obtained for each recruiting site. The list of sites, Ethical Committees, approval numbers and approval dates can be found on the website: <https://www.center-tbi.eu/project/ethical-approval>.

Data sharing: Individual patient data contained within the CENTER-TBI database are not publicly available but permissions for access can be requested at <https://www.center-tbi.eu/data>. We are committed to sharing all other anonymised individual participant and patient data that would support the clinical community. All shareable items are available immediately upon publication and indefinitely, or ending 5 years following article publication, by reasonable request from the Lead Author at ninar@mrc-lmb.cam.ac.uk. Shareable items will be available to anyone who wishes to access them and for any purpose. Code for statistical modelling is provided in Supplementary Appendix 5.

Transparency: The lead author (NMR) affirms that the manuscript is an honest, accurate, and transparent account of the study being reported; that no important aspects of the study have been omitted; and that any discrepancies from the study as planned have been explained.

Copyright: The Corresponding Author has the right to grant on behalf of all authors and does grant on behalf of all authors, an exclusive licence (or non-exclusive for government employees) on a worldwide basis to the BMJ Publishing Group Ltd to permit this article (if accepted) to be published in BMJ editions and any other BMJ PGL products and sublicences such use and exploit all subsidiary rights, as set out in our licence.